Journal of Petroleum Exploration and Production Technology
https://doi.org/10.1007/s13202-024-01787-7

ORIGINAL PAPER-PRODUCTION GEOLOGY

Wettability evaluation of shale oil reservoirs and its impact on the post-fracturing shut-in duration of horizontal wells: a quantitative study for Ordos Basin, NW China

Qihong Lei[1,2,3] · Shuwei Ma[1,2] · Jian Li[2,3] · Youan He[1,2] · Tianjing Huang[1,2] · Wenlian Xiao[4] · Bo Wang[1,2] · ChangChun Liu[2,3]

Received: 8 November 2023 / Accepted: 9 March 2024

Abstract

Shale oil development in Ordos Basin, China, primarily relies on the displacement of crude oil during the post-fracturing shut-in stage (PFSIS) of horizontal wells. Reservoir wettability significantly influences the shut-in duration and even the development approach. However, due to strong heterogeneity and super tight characteristics, the reservoir usually shows an mixed wettability, and it was usually hard to differentiate the wettability in different pore sizes. With this in mind, this study focuses on core samples from shale oil reservoir in the Longdong region of the Ordos basin to quantitatively analyze the reservoir wettability. Amott method combined with nuclear magnetic resonance is adopted in the paper to meed this end. And the optimal post-fracturing shut-in duration for Huachi and Heshui areas in the Longdong region are determined based on both wettability and field practice analysis as well as numerical simulations. Qualitative wettability evaluation reveals that the reservoir in the Longdong region is weakly oil-wet (oil-wet pores account for 58.9% and water-wet pores for 41.1%), and that larger pores are more water-wet, while smaller pores are more oil-wet. Field practice observes a noticeable two-stage decline in wellhead pressure, with pressure drop rates and water content decline rates following the order of neutral reservoir > weakly oil-wet reservoir > oil-wet reservoir during the post-fracturing shut-in stage. Numerical simulations indicate that the determination of the optimal post-fracturing shut-in duration for horizontal wells should consider reservoir properties, wettability, and injection volume. The final optimal shut-in durations for the Huachi and Heshui areas in the reservoir are determined to be 36 days and 43 days, respectively. Our study qualitatively distinguishes the wettability in different pores sizes and thus determines reasonable post-fracturing shut-in durations in different areas in Longdong region. The research has major implication for building a realistic method of wettability analysis in shale or tight oil reservoir.

Keywords Shale oil reservoir · Wettability · Post-fracturing shut-in duration · Ordos Basin

List of symbols

C	Conversion coefficient (ms/μm)
E_o	Total extraction extent during self-imbibition of oil and oil-flooding
$E_{od\text{-}rj}$	Extraction extent of water under oil-flooding for the j-th pore throat under imbibition
E_{oi}	Water extraction extent at the i-th pore throat under oil imbibition and oil-flooding
$E_{os\text{-}ri}$	Extraction extent of water after oil self-imbibition for the i-th pore throat
E_w	Total extraction extent during self-imbibition of water and water-flooding
$E_{wd\text{-}rj}$	Extraction extent of oil under water-flooding for the j-th pore throat under imbibition
E_{wi}	Oil extraction extent at the i-th pore throat under water imbibition and water-flooding

✉ Shuwei Ma
shuwei.ma@hotmail.com

1 Research Institute of Exploration and Development, PetroChina Changqing Oilfield Company, Xi'an, China

2 Petrochina Changqing Oilfield Company, Xi'an, China

3 Longdong Oil and Gas Development Branch, Petrochina Changqing Oilfield Company, Qingyang, China

4 National Key Laboratory of Oil and Gas Reservoir Geology and Exploration, Southwest Petroleum University, Chengdu, China

Published online: 12 April 2024

$E_{ws\text{-}ri}$	Extraction extent of oil after water self-imbibition for the *i*-th pore throat
I_i	Relative wettability index for each pore throat level
$m_{(ri)ao}$	Signal amplitude after self-imbibition of oil for the *i*-th pore throat
$m_{(ri)aw}$	Signal amplitude after self-imbibition of water for the *i*-th pore throat
$m_{(ri)bo}$	Signal amplitude before self-imbibition of oil for the *i*-th pore throat
$m_{(ri)bw}$	Signal amplitude before self-imbibition of water for the *i*-th pore throat
$m_{(rj)a}$	Signal amplitude after self-imbibition of oil-flooding for the *j*-th pore throat
$m_{(rj)ad}$	Signal amplitude after self-imbibition of water-flooding for the *j*-th pore throat under imbibition
$m_{(rj)ao}$	Signal amplitude after self-imbibition of oil-flooding for the *j*-th pore throat under imbibition
$m_{(rj)b}$	Signal amplitude before self-imbibition of water-flooding for the *j*-th pore throat
$m_{(rj)bd}$	Signal amplitude before self-imbibition of water-flooding for the *j*-th pore throat under imbibition
$m_{(rj)bo}$	Signal amplitude before self-imbibition of oil-flooding for the *j*-th pore throat under imbibition
r	Pore throat radius (μm)
$r_{\max}$	Maximum pore throat radius of the rock sample (μm)
$r_{\min}$	Minimum pore throat radius of the rock sample (μm)
$ri_{\max}$	Maximum radius of the *i*-th pore throat (μm)
$ri_{\min}$	Minimum radius of the *i*-th pore throat (μm)
$rj_{\max}$	Maximum radius of the *j*-th pore throat under imbibition (μm)
$rj_{\min}$	Minimum radius of the *j*-th pore throat under imbibition (μm)
T_2	Transverse relaxation time (ms)
V_{wso1}, V_{osw1}	Volume of extracted oil or water during self-imbibition of water or self-imbibition of oil (mL)
V_{wso2} and V_{osw2}	Volume of extracted oil and water during water or oil flooding (mL)
V_{wfo2} and V_{ofw2}	Volume of self-imbibed water and oil after modification based on contribution diagrams (mL)
W_o	Oil wettability index after modification at each pore throat level
W_{oi}	Oil wettability index at each pore throat level
W_w	Water wettability index after modification at each pore throat level
W_{wi}	Water wettability index at each pore throat level
η_d	Percentage of displacement contribution
η_s	Percentage of imbibition contribution

Abbreviations

CTS	Cast thin sections
NMR	Nuclear magnetic resonance
PFSIS	Post-fracturing shut-in stage
PFSID	Post-fracturing shut-in duration
SEM	Scanning electron microscope

Introduction

Wettability is one of the critical parameters for reservoir rocks in oil and gas fields. It influences distribution of pore fluids, determines the microscale displacement efficiency of rocks, and plays a significant role in formulating and implementing recovery strategies, as well as evaluating parameters such as permeability and saturation (He and Tang 2011; Anderson 1986; Tiab and Donaldson 2004; AL-Dujaili et al. 2023a, b). Currently, shale oil development in Ordos Basin relies on natural energy development, that is the imbibition-displacement process of fracturing fluids, to develop crude oil (Zhiyu et al. 2021). Therefore, identifying the wettability of shale oil reservoirs provides a foundation for understanding the fluid flow mechanisms and development approaches.

Common methods for determining wettability include the contact angle method, centrifugation (USBM), spontaneous imbibition (Amott), automatic imbibition, and the Amott-USBM combination method (Bobek et al. 1958; Sutanto et al. 1990; Anderson 1986; Donaldson et al. 1969; Yan 2001). Among these, the Amott spontaneous imbibition method is widely used for wettability assessment in laboratory experiments. It relies on the differences in interfacial energy between rock, water, and oil (Brown and Fatt, 1956). One liquid is more likely to wet the rock surface than the other does and can spontaneously displace the other. By comparing quantities of capillary imbibition of oil (spontaneous imbibition of water) at the presence of residual oil (bound water), the relative wettability index is calculated (Minh et al. 2015; Chen et al. 2020; Huang et al. 2021). The wettability is determined based on the distribution range of the relative wettability index (Borgia et al. 1991; Howard 1998; Zhong et al. 2013; Wang et al. 2018; AL-Dujaili et al. 2023a, b). However, this method shows several limitations: (1) precision of the experiment relies on the volume measurement of oil and water imbibed, and the graduated tube

hardly meet the required precision. (2) The Amott spontaneous imbibition method primarily focuses on the relative sizes of capillary imbibition of oil and water under the influence of capillary forces, neglecting the imbibition effects during water and oil displacement processes, leading to overestimation of wettability. (3) The Amott spontaneous imbibition method is more suitable for evaluating the macroscopic wettability of rock samples, i.e., whether they are oil-wet or water-wet, but cannot assess the wettability of different pore-scale spaces.

With continuous development of nuclear magnetic resonance (NMR) technology, low-field NMR has become a vital geophysical logging method. Due to its unique ability to identify fluid properties, it has been widely used in wettability characterization (Wang et al. 2016, 2018; Xing et al. 2021; Zhao et al. 2021; Xiao 2023).

Petrophysical characterization of shale formations also interested researcher in the USA, due to the increasingly importance of the unconventional resources. They found that acyclic pore model is the one that can most describe spatial distribution of throat sizes (Sakhaee-Pour, and Bryant 2012, 2015; Zapata, and Sakhaee-Pour 2016; Tran, and Sakhaee-Pour 2018a, b, 2019; Yu et al. 2018), among which tree-like pore model is the most applicable to the core-scale measurements(Tran and Sakhaee-Pour 2019), because this model was able to account for the non-plateau-like trend of the drainage during capillary pressure measurement of the shale cores (Sakhaee-Pour and Bryant 2015). Sakhaee-Pour and Li (2016) analyzed drainage experiments conducted on cores and found that the fractal dimension is on the order of 3.1–5.3 for the different shales, reflecting the complexity pore space structure of shale cores. Alessa et al. (2021) explored the pore-throat size and pore-body size distributions of Midra shale in Qatar by measuring capillary pressure and found that unlike the nonplateau-like trend in US shales, Midra shale showed a plateau-like trend, and the pore-throat size has a narrow distribution with an average of close to 22 nm. Machine learning was also adapted by Kasha et al. (2022) to narrow the gap between J curves and allowed an accurate scaling of capillary pressure, providing a very useful way to evaluate the capillary pressure when experiment data are unavailable.

This study proposes a new approach for Amott wettability assessment based on NMR technology to address the limitations of the Amott method. It combines traditional Amott spontaneous imbibition with NMR technology, calculating the extent of fluid extraction at different pore throat scales during the imbibition and the displacement processes relying on capillary imbibition. This calculates the water wetness index, oil wetness index, and relative wettability index for various pore throats. The wettability of different pore throat levels in rock samples is determined based on the relative wettability index. This approach aims to establish a quantitative wettability characterization method for shale oil reservoirs with complex mineral compositions and pore structures, providing guidance for the formulation of shale oil development policies.

Geological setting

Geological overview

Shale oil in the Triassic Chang 7 member of the Mesozoic era in Ordos Basin is primarily controlled by the semi-deep lake to deep lake gravity flow sedimentary system (Fig. 1). The co-genetic pattern of fine-grained sandstone and mud shale, widely distributed, is influenced by ancient climate, topography, and water depth, controlled by gravity flow deposits developed in the steep slope belts and central basin, and deltaic deposits in the gentle slope belts. The sweet spots of shale oil are controlled by ultra-rich organic matter supplying hydrocarbons, large-scale rich sand in deep water, co-storage in micro and nanometer pores and throats, and high-intensity continuous injections. The medium-thin layers of silt-fine sandstone held within thick mud shale layers are the primary targets for cost-effective shale oil

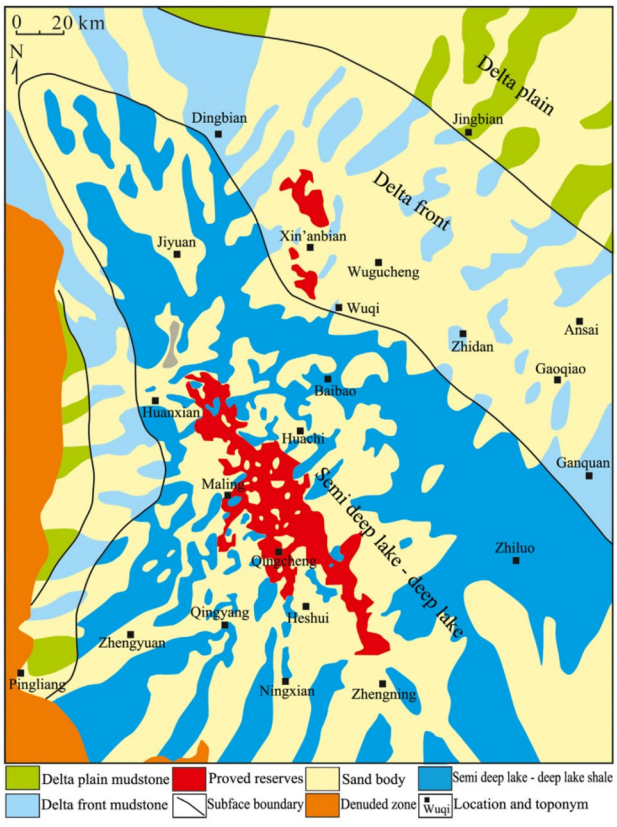

Fig. 1 Shale oil exploration results in the Ordos Basin (modified from Fu, 2022)

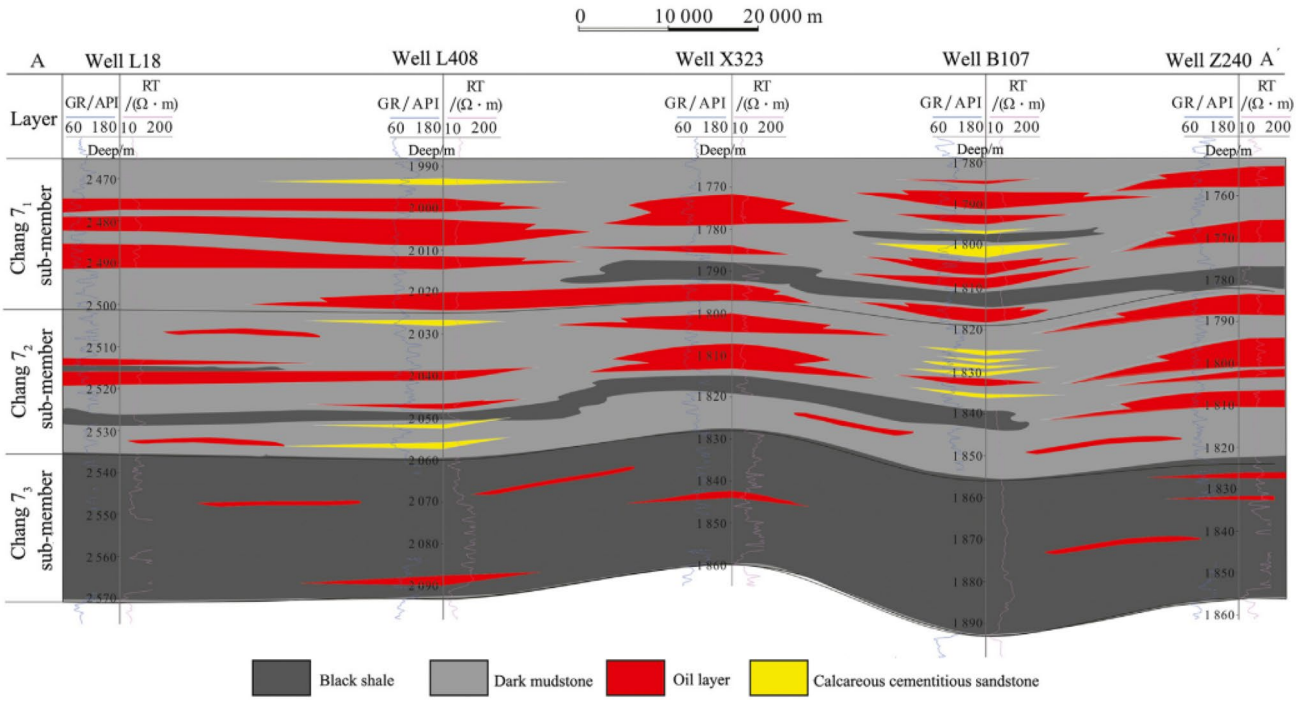

Fig. 2 Shale oil profile of Chang 7 Member in Qingcheng Oilfield (modified from Fu, 2022)

development (Yang et al. 2021; Fu et al. 2018, 2019, 2021) (Fig. 2). The pressure coefficient of the Chang 7 stratum in the Ordos Basin ranges from 0.7 to 0.8, making it a typical low-pressure basin. The crude oil has characteristics of low density (0.73–0.78 g/cm^3), low viscosity (1.36–1.47 mPa·s), low freezing point (15.68–16.33 °C), and lack of sulfur. Overall, it is considered light crude oil. The initial gas-oil ratio ranges from 90 to 110 m3/t, and the high gas-oil ratio reduces the viscosity and density of shale oil, which is key to the cost-effective development of low-pressure shale oil in the Chang 7 member.

Development status

Before 2011, the Chang 7 section was primarily studied as a source rock. Sparse exploration had identified several oil-rich areas. However, after direct well fracturing, poor trial pumping and rapid production decline made it economically unviable for extraction. From 2011 to 2017, Changqing Oilfield made a significant paradigm shift in the understanding of the Chang 7 shale layer system, transitioning from viewing it as "solely a source rock" to an integrated "source and reservoir." Drawing from North American shale oil exploration and development concepts, with "horizontal drilling + volume fracturing" as the breakthrough, trials were carried out in the West 233 well area, Zhuang 183 well area, and Ning 89 well area. The initial daily production of the trial area was 12.8 tons, with a yearly production of 3,970 tons in the first year. Currently, the average daily production is 4.7 tons per well, with a cumulative production of 23,000 tons, marking a breakthrough in daily and cumulative production. This proves that refining horizontal drilling with volume fracturing can further enhance production, proving crucial for efficient extraction of interbedded shale oil. Since 2018, it has entered a phase of large-scale development with dense well deployments and factory-like operations. Since 2018, a total of 511 horizontal wells have been put into production in Qingcheng Oilfield, with an average horizontal section length of 1679 m, an average oil layer encounter rate of 77.0%, an average of 24 fracturing stages per well, an injected fluid volume of 27,000 cubic meters, and a sand addition volume of 2975 cubic meters. For the 350 horizontal wells that have been in production for three months, the initial daily oil production is 13.6 tons, with a water cut of 35.2%, reaching a daily production of 12.3 tons in the year of production. The first-year average cumulative production is 4430 tons, with a forecasted 20-year EUR value of 26,000 tons.

Data and method

Experimental samples

Samples were selected from shale oil reservoirs of Chang7 member in Huachi and Heshui areas of the Longdong region

Table 1 Basic physical properties of experimental rock samples

Sample No.	Area	Length (mm)	Diameter (mm)	Density (g/cm^3)	Porosity (%)	Permeability (mD)
1	Huachi	50.17	25.27	2.432	8.26	0.237
2		50.09	25.32	2.439	9.26	0.215
3	Heshui	50.12	25.11	2.441	8.57	0.195
4		50.11	25.19	2.440	8.96	0.203

in Ordos basin. Porosity range of the samples is from 8.26% to 9.26% and permeability between 0.195 and 0.237 mD (Table 1). Wettability experiments based on the NMR technology using a simulated formation water with a 20,000 ppm concentration of $MnCl_2$ solution. The oil used in the experiment is crude oil from the same member.

Observation of core cast thin sections (CTS) and scanning electron microscope (SEM) found that the lithology of the reservoir in the study area includes very fine to fine-grained feldspar lithic sandstone, and fine-grained lithic sandstone. Clastic rock composition is primarily dominated by quartz and feldspar, with a certain amount of rock fragments and other clasts. It exhibits a high quartz and low feldspar characteristic, with pore-filling materials mainly composed of illite, calcite, and dolomite. The overall porosity of the region is moderately developed, predominantly consisting of dissolution pores, including feldspar dissolution pores and residual pores (Fig. 3a, b). The overall porosity of the rock samples ranges from 4.6% to 7% (Fig. 3c). SEM analysis reveals a widespread distribution of clay minerals on the reservoir pore and throat surfaces, with illite being the primary component, and relatively fewer water-sensitive minerals.

Experimental instruments

Amott spontaneous imbibition experiments combined with nuclear magnetic resonance (NMR) technology were conducted using deuterium oxide (heavy water) and reservoir crude oil. This allowed for an accurate determination of imbibition oil (water) volumes and displacement oil (water) volumes from NMR spectra at different stages. It characterized the wettability features within different pores. By comparing the volume ratio of self-imbibed water displacing oil (or self-imbibed oil displacing water) to the total displaced oil (or oil–water), wettability of the samples was determined (Fig. 4).

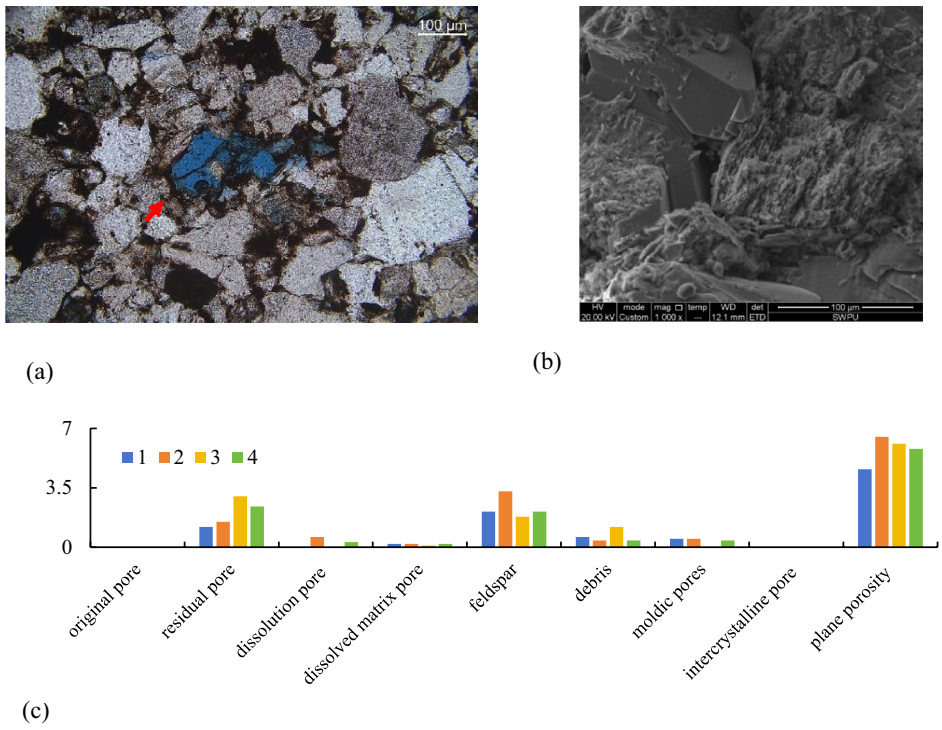

Fig. 3 CTS and SEM Images, and Statistics for Huachi and Heshui Areas **a** Sample-1 for sandstone lithoclast dissolution pores; **b** Sample-3 for quartz filling, feldspar dissolution; **c** Statistics of Porosity Type

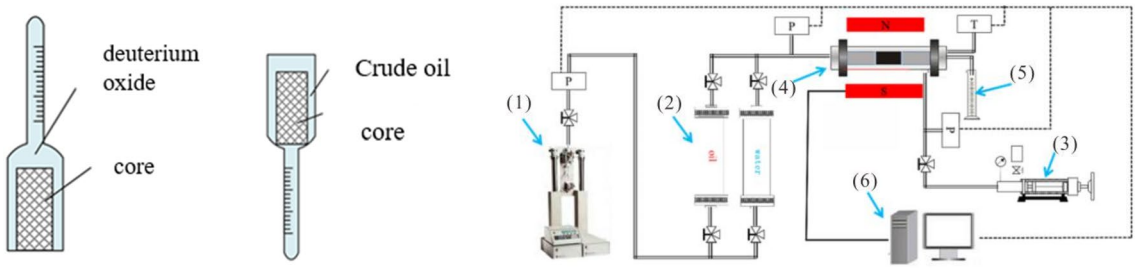

Fig. 4 Experimental Setup by Amott Method Combined with NMR (1)High pressure displacement pump; (2) Oil and water container; (3)Confining pressure pump;(4) Core holder; (5) Fluid collector; (6) NMR instrument

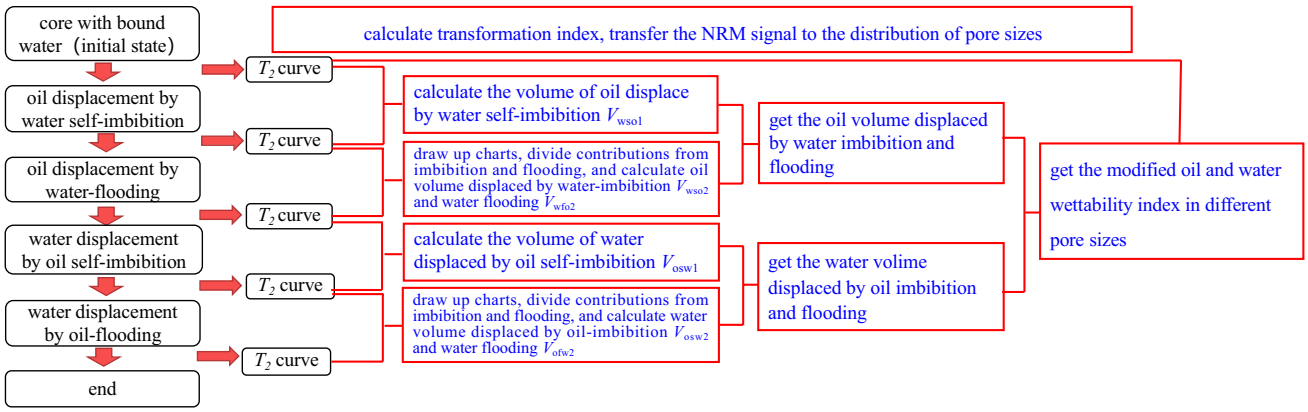

Fig. 5 Schematic of the wettability experiment based on nmr Amott spontaneous imbibition method

Experimental procedures

The experimental procedures for this study, as shown in Fig. 5, were as follows:

1. A cylindrical rock core with a length of 7–8 cm from the shale oil reservoir was selected, cleaned, and dried. The dry weight (m_0), porosity (φ_{He}), and permeability (k) of the core were measured. It was then cut into three sections: Sections I and II were 1–2 cm in length, while Section III was 4–5 cm.
2. High-pressure mercury injection experiments were conducted on the Section II, following the national standard GB/T 29171-2012 "Determination of Mercury Intrusion Porosimetry Curve of Rocks" to obtain pore throat radius and distribution data.
3. Section III of the core underwent a vacuum pressure saturation experiment using formation water. Initially, the core was evacuated to 133 Pa, and then it was pressurized with a 20 MPa formation water for 48 h. Mass of Section III was measured (m_1), and effective pore volume (V_{eff}) and effective porosity (φ_{eff}) were calculated. When the relative difference between φ_{eff} and φ_{He} was less than 2%, the core was considered fully saturated. Otherwise, the saturation process was repeated following the above steps. Simultaneously, the NMR instrument was initiated, and parameters were set to measure the NMR T_2 spectra of the saturated water in Section III.
4. Section III, saturated with water, was placed in a core holder, and the displacement process was initiated. Deuterium oxide (heavy water) was used to displace the saturated water in Section III. The NMR T_2 spectra during the displacement process were monitored until there were no signal responses.
5. Formation crude oil was used to displace the heavy water-saturated Section III to establish a bound water saturation. Subsequently, the core was aged for one week under formation temperature, and the NMR T_2 spectra were measured after aging.
6. The aged Section III was placed in a water uptake apparatus filled with deuterium oxide, and self-imbibition of water and oil displacement were conducted. The self-imbibition experiment was considered complete when the water uptake and oil displacement remained stable for 24 consecutive hours. The water uptake and oil displacement volumes (V_{o1}), and the T_2 spectra of the sample were measured.

7. Section III, after self-imbibition, was placed in a core holder, and heavy water was used to displace the core until the exit end reached a water saturation of 99.95%. This marked the end of the water-flooding experiment, and water displacement volumes (V_{o2}) and the T_2 spectra of the sample were recorded.
8. Crude oil was filled in an oil uptake apparatus, and the oil-saturated Section III was placed in a bottle for self-imbibition and oil drainage experiments. The self-imbibition experiment was considered complete when the self-imbibition and oil drainage remained stable for 24 consecutive hours. The self-imbibition oil drainage volume ($Vw1$) and the T_2 spectra of the rock sample were measured.
9. Section III, after self-imbibition, was placed in a core holder, and formation oil was used to displace the core until the oil saturation at the exit end reached 99.95%. This marked the end of the displacement experiment, and the oil displacement volume (V_{w2}) and the T_2 spectra of the sample were recorded.
10. The pore throat distribution curve obtained from high-pressure mercury injection and the NMR T_2 spectra under complete water saturation were plotted on the same coordinate system for scale comparison. This allowed the conversion coefficient between NMR T_2 time and pore throat radius to be determined, enabling the transformation of the NMR T_2 spectrum into the corresponding pore throat distribution curve.

Results and discussion

Qualitative evaluation of wettability

Spontaneous imbibition method

Under the influence of capillary pressure, wetting fluids possess the characteristic of spontaneously imbibed into the rock pores and displacing non-wetting fluids. By measuring and comparing the quantities of capillary imbibition of oil (or spontaneous imbibition of water) in the presence of residual oil (or bound water) in reservoir rocks and the displacement of oil by water (or displacement of water by oil), the wettability of reservoir rocks to oil (or water) can be determined (Brown, 1956). The wettability was evaluated using the spontaneous imbibition method for 13 samples from the Huachi area and 12 samples from the Heshui area in Ordos Basin. The results indicate that reservoirs of Huachi area are oil-wet, while that in Heshui area show weakly oil-wet, and the overall basin exhibits weakly oil-wet characteristics (Table 2) (standards refer to "Appendix").

Table 2 Wettability results of reservoirs in the Longdong region using the spontaneous imbibition method

Area	Sub-member	Depth (m)	Number of samples	Porosity (%)	Spontaneous imbibition method					
					Volume of oil displaced by water imbibition (%)	Volume of water displaced by oil imbibition (%)	Oil wettability index (W_o)	Water wettability index (W_w)	Relative wettability index (W_w-W_o)	Wettability
Huachi	$Chang7_1$ $Chang7_2$	2142.4	13	9.9	13.11	43.51	0.43	0.13	−0.3	Oil wet
Heshui	$Chang7_1$ $Chang7_2$	1793.2	12	9.1	14.04	42.34	0.42	0.13	−0.28	Weakly Oil wet
Average		1974.8	25	9.4	13.6	41.9	0.42	0.14	−0.28	Weakly Oil wet

Contact angle method

At three-phase junction of a water–oil–solid system, equilibrium relationship of surface energies follows the Young–Laplace equation, and the size of the contact angle is related to the wetting degree of the solid by oil and water (Washburn 1921; Al-Dujaili et al 2023a, b). Therefore, measuring the contact angle of the oil–water-reservoir rock system provides insights into the wettability of oil and water on the reservoir rock surface. During this contact angle test, actual reservoir rock samples provides a more realistic representation of the reservoir. Three modes were set up: (1) dry samples (without oil washing); (2) samples 100% saturated with water; (3) samples saturated with oil and water (oil saturation between 55 and 70%). Oil and water were dropped onto the rock surface, and the contact angles of the oil droplets and water droplets on the rock surface were measured. Results showed that in all states, the contact angle of oil is < 10°, and that of water ranges from 37.3° to 73.6°, indicating that the Chang 7 reservoir exhibits an oil wet (Fig. 6) (National Development and Reform Commission, 2007).

Quantitative evaluation of wettability using NMR-based Amott spontaneous imbibition method

Wettability calculation

Conversion coefficient between NMR T_2 time and pore throat radius is calculated using Eq. (1) (Yang et al. 2013):

$$T_2 = Cr \tag{1}$$

where T_2 is the transverse relaxation time (ms), C is the conversion coefficient (ms/μm), and r is the pore throat radius (μm).

During the experiment, heavy water was used to shield the NMR signal of the water. Therefore, the obtained T_2 spectrum represents only the signal from oil. Changes in T_2 spectrum reflect variations in the oil phase within the experimental core. Hence, extent of extraction for various pore throat levels during self-imbibition of water and self-imbibition of oil drainage processes can be calculated using Eqs. (2) to (3) (modified from Yang et al. 2023):

$$E_{ws-ri} = \frac{\int_{ri_{\min}}^{ri_{\max}} m(r_i)_{bw}\mathrm{d}r_i - \int_{ri_{\min}}^{ri_{\max}} m(r_i)_{aw}\mathrm{d}r_i}{\int_{r_{\min}}^{r_{\max}} m(r_i)_{bw}\mathrm{d}r_i} \tag{2}$$

$$E_{os-ri} = \frac{\int_{ri_{\min}}^{ri_{\max}} m(r_i)_{ao}\mathrm{d}r_i - \int_{ri_{\min}}^{ri_{\max}} m(r_i)_{bo}\mathrm{d}r_i}{\int_{r_{\min}}^{r_{\max}} m(r_i)_{ao}\mathrm{d}r_i} \tag{3}$$

where $E_{ws\text{-}ri}$ is the extraction extent of oil after water self-imbibition for the i-th pore throat, $E_{os\text{-}ri}$ is the extraction extent of water after oil self-imbibition for the i-th pore throat, $ri_{\min}$ is the minimum radius of the i-th pore throat (μm), $Ri_{\max}$ is the maximum radius of the i-th pore throat, μm, $r_{\min}$ is the minimum pore throat radius of the rock sample (μm), $r_{\max}$ is the maximum pore throat radius of the rock sample(μm), $m_{(ri)bw}$ is the signal amplitude before self-imbibition of water for the i-th pore throat, $m_{(ri)aw}$ is the signal amplitude after self-imbibition of water for the i-th pore throat, $m_{(ri)bo}$ is the signal amplitude before self-imbibition of oil for the i-th pore throat and $m_{(ri)ao}$ is the signal amplitude after self-imbibition of oil for the i-th pore throat.

The next step is to create contribution diagrams for the imbibition and displacement processes during water and oil flooding. To do that, we first calculate extraction extent under the influence of imbibition at different pore throat sizes during water flooding and oil flooding. When both oil and water phases exist in the pore space, fluid velocity of the displacing phase can be calculated using Eq. (4).

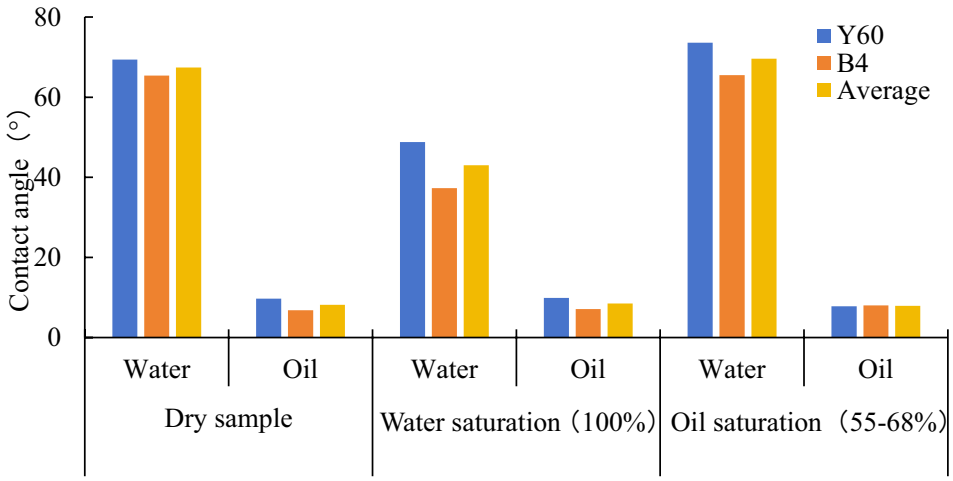

Fig. 6 Contact Angle Tests by Young–Laplace equation for Shale Oil Reservoirs in the Ordos Basin

Equation (4) obtains the fluid velocity under imbibition and displacement processes. Then, contributions of imbibition and displacement at different pore throat radii can be calculated using Eqs. (4) to (6) (modified from He, 2011) using contact angle of the sample and the displacement pressure applied in the displacement experiment.

$$v_s = \frac{r^2\left(\frac{2\sigma\cos\theta}{r}\right)}{8\mu_w\sqrt{L^2 - \frac{r^2}{4\mu_o}\left(1-\frac{\mu_w}{\mu_o}\right)\left(\frac{2\sigma\cos\theta}{r}\right)t}} \tag{4}$$

$$v_s = \frac{r^2\left(\frac{2\sigma\cos\theta}{r}\right)}{8\mu_w\sqrt{L^2 - \frac{r^2}{4\mu_o}\left(1-\frac{\mu_w}{\mu_o}\right)\left(\frac{2\sigma\cos\theta}{r}\right)t}} \tag{5}$$

$$v_d = \frac{r^2\Delta p}{8\mu_w\sqrt{L^2 - \frac{r^2}{4\mu_o}\left(1-\frac{\mu_w}{\mu_o}\right)\Delta p t}} \tag{6}$$

And the last step is to create diagrams showing the contribution rates versus pore throat radius (Eqs. (7) to (8)).

$$\eta_s = \frac{\frac{2\sigma\cos\theta}{r}}{\left(\Delta p + \frac{2\sigma\cos\theta}{r}\right)} \tag{7}$$

$$\eta_d = \frac{\Delta p}{\left(\Delta p + \frac{2\sigma\cos\theta}{r}\right)} \tag{8}$$

where η_d is the percentage of displacement contribution, and H_s is the percentage of imbibition contribution, as a decimal.

Based on the contribution diagrams formed above, choose a radius point where the imbibition contribution rate is greater than 0.9 to calculate the extraction extent of various pore throats using NMR T_2 spectrum curves during water and oil flooding processes. The formulas for this calculation are as follows:

$$E_{wd-rj} = \frac{\int_{rj_{\min}}^{rj_{\max}} m(r_j)_{bd}\mathrm{d}r_j - \int_{rj_{\min}}^{rj_{\max}} m(r_j)_{ad}\mathrm{d}r_j}{\int_{r_{\min}}^{r_{\max}} m(r_j)_b\mathrm{d}r_j} \tag{9}$$

$$E_{od-rj} = \frac{\int_{rj_{\min}}^{rj_{\max}} m(r_j)_{ad}\mathrm{d}r_j - \int_{rj_{\min}}^{rj_{\max}} m(r_j)_{bd}\mathrm{d}r_j}{\int_{r_{\min}}^{r_{\max}} m(r_j)_a\mathrm{d}r_j} \tag{10}$$

where:

$E_{wd\text{-}rj}$ is the extraction extent of oil under water-flooding for the j-th pore throat under imbibition,, $E_{od\text{-}rj}$ is the extraction extent of water under oil-flooding for the j-th pore throat under imbibition, $rj_{\min}$ is the minimum radius of the j-th pore throat under imbibition (μm), $rj_{\max}$ is the maximum radius of the j-th pore throat under imbibition (μm), $m_{(rj)bd}$ is the signal amplitude before self-imbibition of water-flooding for the j-th pore throat under imbibition, $m_{(rj)ad}$ is the signal amplitude after self-imbibition of water-flooding for the j-th pore throat under imbibition, $m_{(rj)bo}$ is the signal amplitude before self-imbibition of oil-flooding for the j-th pore throat under imbibition, $m_{(rj)ao}$ is the signal amplitude after self-imbibition of oil-flooding for the j-th pore throat under imbibition, $m_{(rj)b}$ is the signal amplitude before self-imbibition of water-flooding for the j-th pore throat, and $m_{(rj)a}$ is the signal amplitude after self-imbibition of oil-flooding for the j-th pore throat.

Equations (11) to (12) are to calculate the both the oil and water extraction extent by imbibition for each pore throat level during self-imbibition of water and water-flooding processes, and during self-imbibition of oil and oil-flooding.

$$E_{wi} = E_{ws-ri} + E_{wd-rj} \tag{11}$$

$$E_{oi} = E_{os-ri} + E_{od-rj} \tag{12}$$

where E_{wi} is the oil extraction extent at the i-th pore throat under water imbibition and water-flooding, and E_{oi} is the water extraction extent at the i-th pore throat under oil imbibition and oil-flooding.

Total extraction extent during both self-imbibition of water and water-flooding, as well as self-imbibition of oil and oil-flooding, are calculated using Eqs. (13) to (14):

$$E_w = \frac{\int_{r_{\min}}^{r_{\max}} m(r_i)_{bsw}\mathrm{d}r_i - \int_{r_{\min}}^{r_{\max}} m(r_i)_{adw}\mathrm{d}r_i}{\int_{r_{\min}}^{r_{\max}} m(r_i)_{bsw}\mathrm{d}r_i} \tag{13}$$

$$E_o = \frac{\int_{r_{\min}}^{r_{\max}} m(r_i)_{ado}\mathrm{d}r_i - \int_{r_{\min}}^{r_{\max}} m(r_i)_{bso}\mathrm{d}r_i}{\int_{r_{\min}}^{r_{\max}} m(r_i)_{ado}\mathrm{d}r_i} \tag{14}$$

where E_w is the total extraction extent during self-imbibition of water and water-flooding, and E_o is the total extraction extent during self-imbibition of oil and oil-flooding, as a decimal.

Water wettability index, oil wettability index, and relative wettability index for each pore throat level are calculated using Eqs. (11) to (14), and wettability of different pore throats in the samples are determined based on the wettability index in industry standards. And then the wettability index is modified based on the contribution diagrams of imbibition and flooding processes (Eqs. (17) to (18)) (modified from Anderson 1986; Morrow 1990). And in the end, the proportion of oil-wet pores and water-wet pores in the rock sample are calculated.

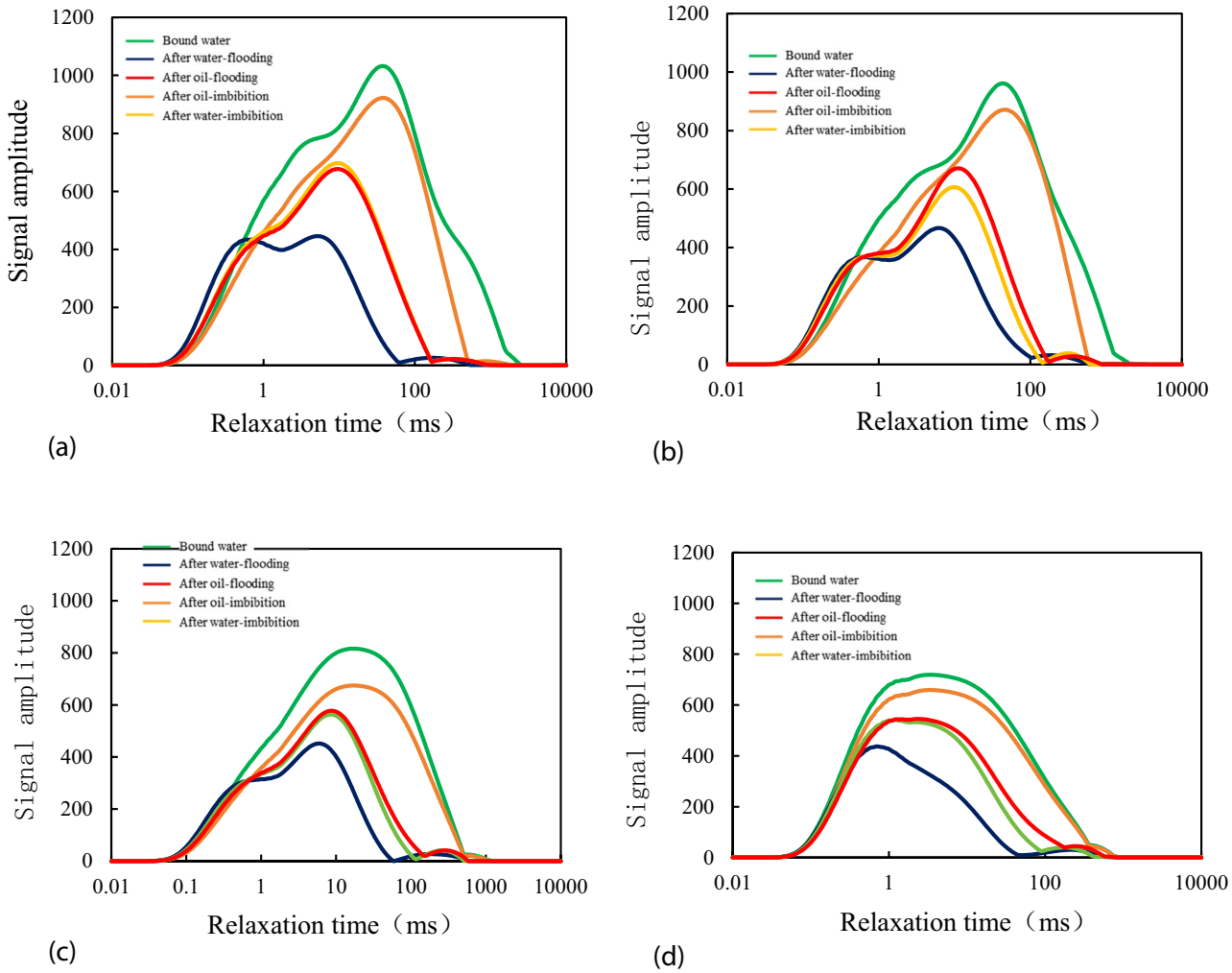

Fig. 7 Nuclear magnetic resonance (NMR) spectra during the spontaneous imbibition process **a** Core-1 self-imbibition process NMR spectrum; **b** Core-2 self-imbibition process NMR spectrum; **c** Core-3 self-imbibition process NMR spectrum; **d** Core-4 self-imbibition process NMR spectrum

$$W_{wi} = \frac{E_{wi}}{E_w} \tag{15}$$

$$W_{oi} = \frac{E_{oi}}{E_o} \tag{16}$$

$$W_w = \frac{V_{wso1} + V_{wso2}}{V_{wso1} + V_{wso2} + V_{wfo2}} \tag{17}$$

$$W_o = \frac{V_{osw1} + V_{osw2}}{V_{osw1} + V_{osw2} + V_{ofw2}} \tag{18}$$

$$I_i = W_w - W_o \tag{19}$$

where W_{wi} is the water wettability index at each pore throat level, W_{oi}: is the oil wettability index at each pore throat level, W_w is the water wettability index after modification at each pore throat level, W_o is the oil wettability index after modification at each pore throat level, V_{wso1} and V_{osw1} are the volumes of extracted oil or water during self-imbibition of water or self-imbibition of oil (mL), V_{wso2}, and V_{osw2} are the volumes of extracted oil or water during water or oil flooding (mL), V_{wfo2} and V_{ofw2} are the volumes of self-imbibed water and oil after modification based on contribution diagrams (mL), and I_i is the relative wettability index for each pore throat level.

Wetting characteristics of different pore throats

Based on the proposed new evaluation processes describing wetting characteristics in different pore spaces, significant

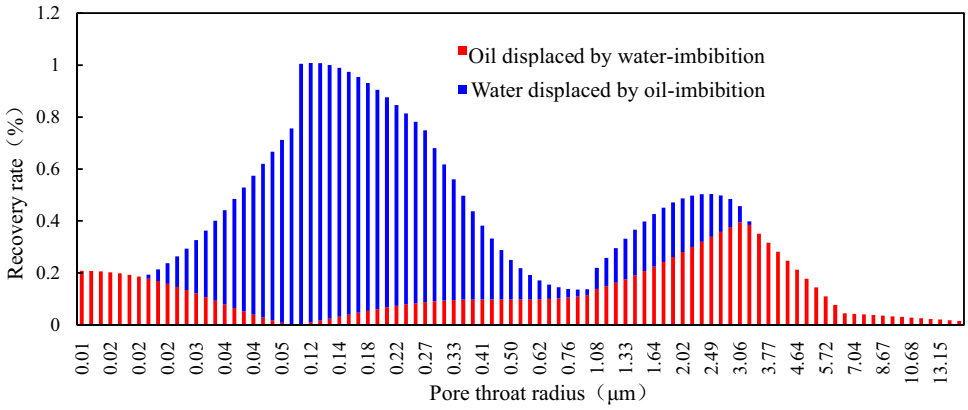

Fig. 8 Extraction extent of different pore spaces in sample 1 during spontaneous water imbibition and spontaneous oil imbibition

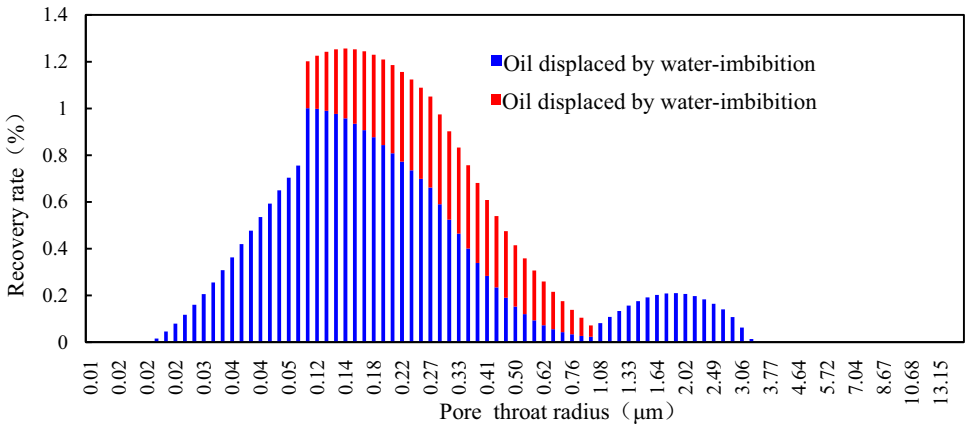

Fig. 9 Imbibition extent during water and oil flooding in sample 1

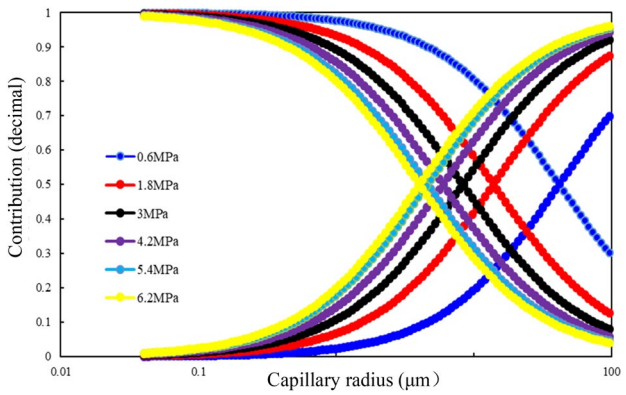

Fig. 10 Imbibition and displacement chart

variations were observed in T_2 spectrum curves before and after water and oil self-imbibition (Fig. 7). This indicates that samples exhibit mixed wetting characteristics. Since capillary imbibition still occurs during displacement processes (Figs. 8, 9) (taking Sample 1 as an example), contribution diagrams for flooding and imbibition were plotted using the formula (Fig. 10). By considering the imbibition recovery during flooding process and modifying the wettability index accordingly, the modified water and oil wettability index were calculated for different pore spaces in the four samples, and corresponding distribution diagrams were generated (Figs. 11, 12, 13, 14, 15).

Figures show that the wetting characteristics in different pore spaces of the studied area's rock exhibit significant variations. In relatively larger pores, water wettability index is generally higher than the oil wettability index, and for some samples, the water wettability index even reaches 1, indicating a strongly water-wet characteristic in these pores. As the pore radius decreases, the oil wettability index increases and gradually surpasses the water wettability index (Samples 1 and 3). Some samples exhibit a "double-peak" feature in their oil wettability index (2 and 4), with oil wettability index peaks at different pore spaces. Overall, oil-wet pores are mainly distributed in the pore radius with a range of 0.1 to 4 μm. Pores with a radius larger than approximately 4–5 μm and smaller than 0.1 μm exhibit significantly lower oil wettability index and are mostly show a water wetting behavior.

Table 3 provides statistics of the proportions of water-wet and oil-wet pores in the micro-pores, meso-pores, and macro-pores within the four rock samples. For samples from the Huachi area (Samples 1 and 2), oil-wet characteristics

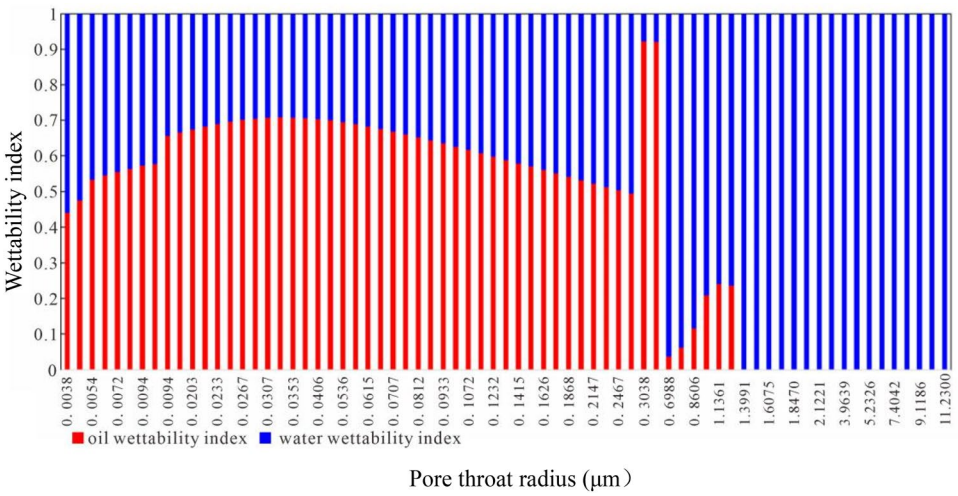

Fig. 11 Wettability evaluation results for different pore spaces in sample 1 after modification

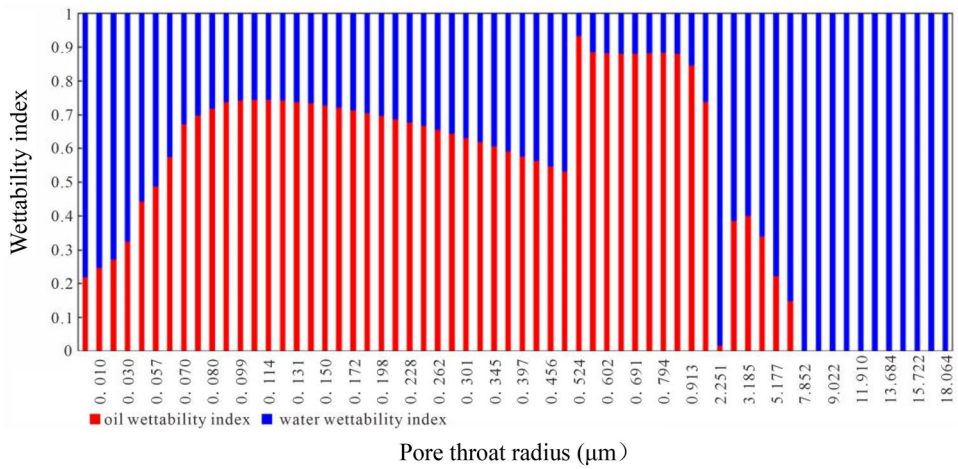

Fig. 12 Wettability evaluation results for different pore spaces in sample 2 after modification

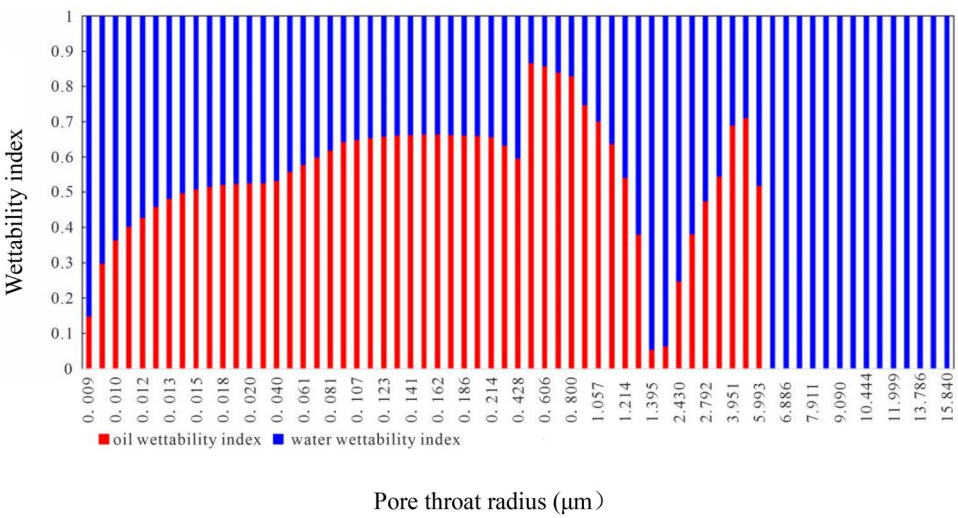

Fig. 13 Wettability evaluation results for different pore spaces in sample 3 after modification

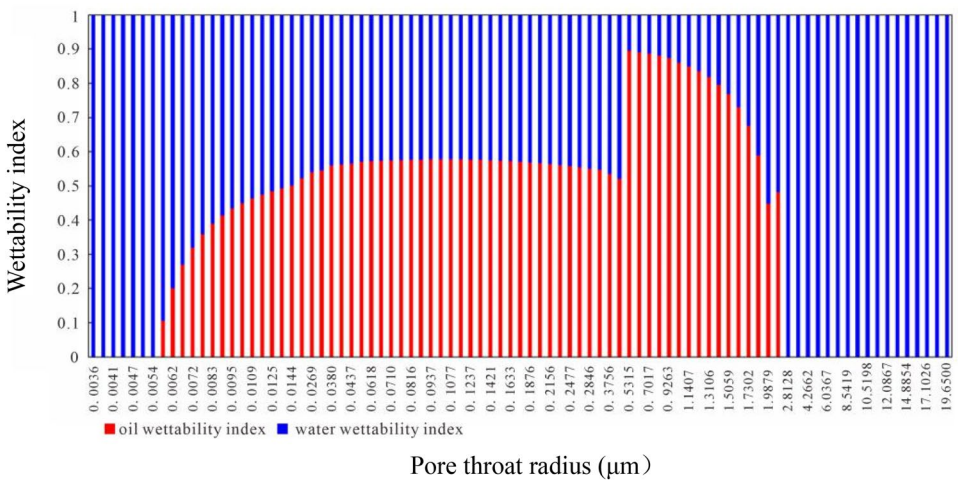

Fig. 14 Wettability evaluation results for different pore spaces in sample 4 after modification

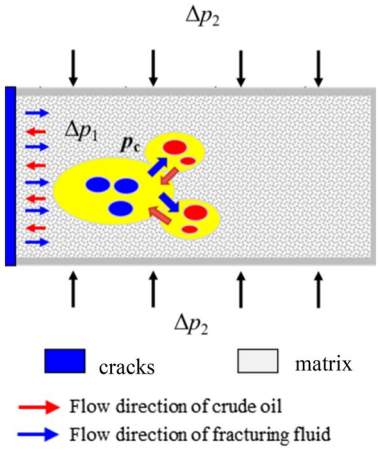

Fig. 15 Flow of oil and water in shale oil reservoir during PFSIS

Table 3 Summary of the proportions of water-wet and oil-wet pores in samples

Area	Sample No.	Water-wet pore (%)	Oil-wet pore (%)
Huachi	1	39.40	60.60
	2	37.10	62.90
Average		38.25	61.75
Heshui	3	43.10	56.90
	4	44.80	55.20
Average		43.95	56.05
Overall average		41.1	58.9

are relative stronger than oil-wet in the micro-pores, with water-wet pores accounting for approximately 38.25% and oil-wet pores for 61.75%. In contrast, samples from Heshui area (Samples 3 and 4) exhibit stronger water-wet characteristics in the micro-pores, with water-wet pores accounting for 43.95% and oil-wet pores 56.05%. Based on the statistical results, the Chang7 reservoir overall exhibits a more oil-wet characteristic(with oil wet pores accounting for 58.9%).

Table 4 Basic parameters of the samples used in dynamic imbibition experiment

Sample No.	Porosity (%)	Permeability (mD)	Injection pressure (MPa)	Total recovery rate (%)
5	10.38	0.122	0	2.21
6	7.51	0.096	1	9.96
7	8.77	0.111	3	37.52
8	7.43	0.127	6	44.64

Mechanism of imbibition processes in the reservoir

After years of practices in shale oil development in Ordos Basin, a development approach has gradually emerged, known as "long horizontal wells—large-scale volume fracturing—post-fracturing shut-in—backflow" (Jiao 2021). During PFSIS, crude oil is extracted by the imbibition and displacement of fracturing fluid and reservoir fluid in the pore spaces (Zhiyu et al. 2021). During fracturing and PFSIS, pressure around the near-wellbore zone is much higher than the formation pressure. Some fracturing fluid enters large pores under this pressure differences (displacement), while some enters small pores due to capillary pressure (imbibition) (Wan et al. 2023). As pressure propagate and water saturation changes, the displacement process gradually weakens, and imbibition becomes relatively strong (Fig. 15).

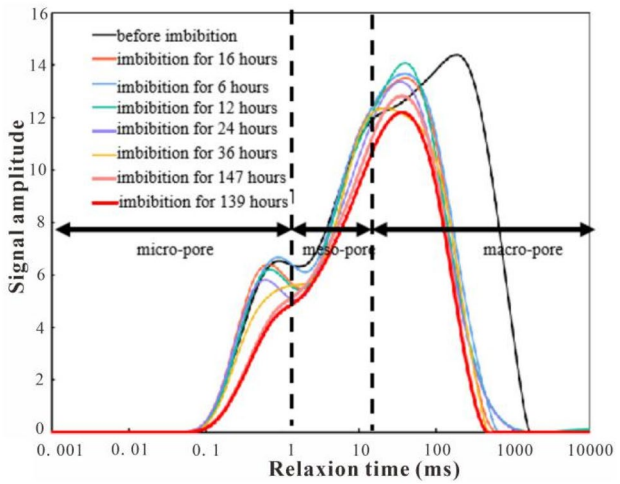

Fig. 16 Nuclear magnetic resonance (NMR) T_2 spectrum during the dynamic imbibition process of Sample 7

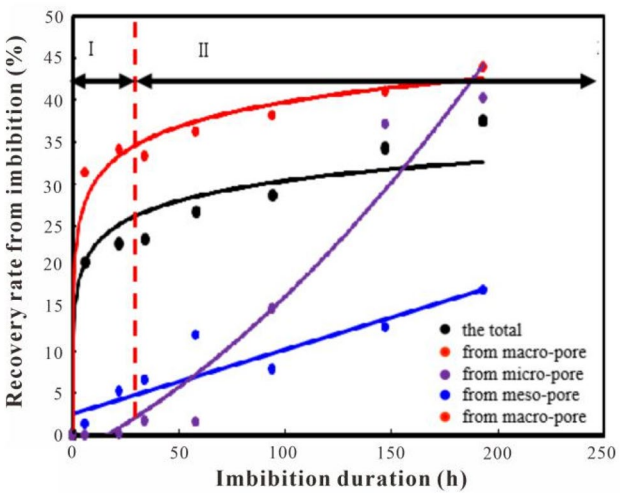

Fig. 17 Imbibition curves for different pore spaces at different imbibition stages

Physical simulation of oil production characteristics during the PFSIS of shale oil wells

To investigate oil production characteristics in different pore throat sizes during PFSIS, samples from Longdong region were used to simulate dynamic imbibition under reservoir conditions at different injection pressures during PFSIS.

During the experiment, real-time data were collected, including NMR T_2 spectra, injection pressure, and imbibition time. T_2 figures were drawn before and during the experiment. The rock sample properties and experimental recovery rates are shown in Table 4, and the NMR T_2 spectra during the imbibition process are displayed in Fig. 14.

T_2 spectra peaks of the small and large pores gradually decrease with increasing imbibition time, and the relaxation times corresponding to pore sizes in the range of 1–10 ms only show small fluctuations, indicating that during the imbibition process, the small and large pores are effectively active. Pore size with the relaxation times corresponding to 1–10 ms are acting as channels connecting the small and large pores (Xiao et al. 2021). Taking sample 7 as an example (Fig. 16), NMR T_2 spectrum of the core in bound water state exhibits a "double-peak" feature, with the signal amplitude peak of the short relaxation time (T_2 between 0.01 and 5.94 ms) being smaller than that of the long relaxation time (T_2 between 5.94 and 219 ms). On the one hand, this indicates that the distribution of crude oil in the reservoir core exhibits strong non-uniformity, and on the other, crude oil is primarily located in the medium to large pores. After 16 h of imbibition, decrease of NMR signal in the core mainly comes from pores corresponding to T_2 values greater than 10 ms, and with the increase of imbibition time, crude oil in pores corresponding to relaxation times less than 10 ms start to flow.

Figure 17 shows the recovery curves of different pores as a function of imbibition time. It shows that the recovery rate in the large pores, mainly in water-wet pores, increases rapidly initially, while the recovery rate in the medium and small pores, mainly oil-wet pores, increases relatively slowly. With a longer imbibition time, the recovery rate in the large pores stabilizes, while the recovery rate in the medium and small pores, especially the small pores, increases rapidly.

Optimization of post-fracturing shut-in duration (PFSID) among different areas

Pressure characteristics during the PFSIS in the Chang 7 shale oil reservoir and its relationship with reservoir wettability

Extensive field development practices have revealed that a very short PFSID leads to unstable reservoir pressure diffusion and increased sand production, while an overly PFSID results in an increased viscosity of crude oil, wellbore scaling, and other issues that can impact well productivity. It has been observed that the bottom hole pressure stabilizes after approximately 30 to 40 days. In the case of Chang 7 shale oil reservoir in Ordos Basin, wellhead pressure change

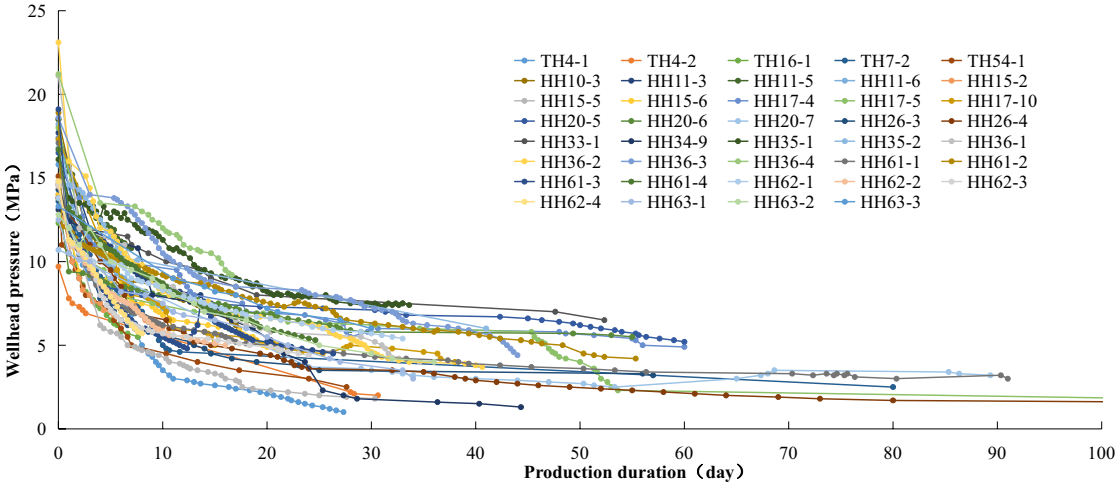

Fig. 18 Relationship between wellhead pressure decline curve and time during the shut-in process of intermittent horizontal shale oil wells (Wan, 2023)

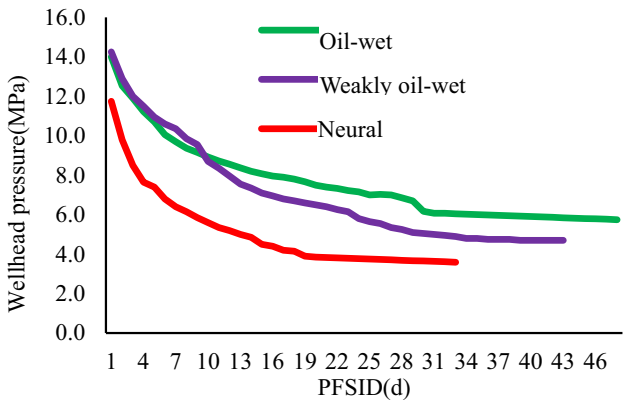

Fig. 19 Relationship between PFSID and pressure decline curve under different Wettability

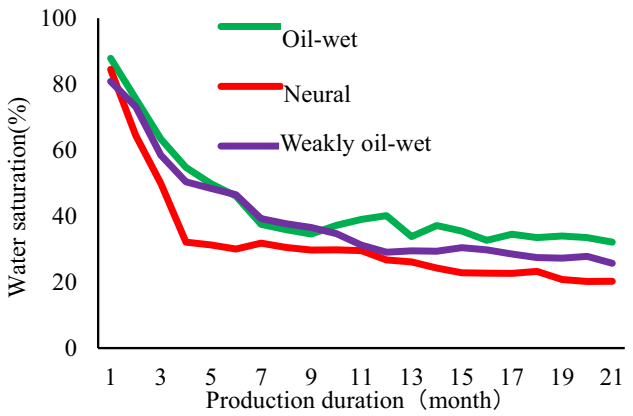

Fig. 20 Decline curves of water saturation in daily production for different wettability

undergoes two distinct phases during PFSIS (Fig. 18): a rapid decline phase (with a pressure drop rate greater than 0.5 MPa/day) and a slow decline phase (with a pressure drop rate ranging from 0.1 to 0.5 MPa/day) (Wan et al., 2023). These phases correspond to rapid and slow stages of imbibition, respectively. When the pressure drop rate exceeds 0.5 MPa/day, it indicates that PFSIS is in the pressure expansion phase. When the pressure drop rate ranges from 0.1 to 0.5 MPa/day, it suggests that the PFSIS is in the oil–water displacement phase (Wan et al. 2023). The PFSIS is considered to be ended when the pressure curve stabilizes, with a continuous pressure drop rate less than 0.1 MPa/day for three consecutive days (Wan et al. 2023).

The PFSID, water-cut decline curves, pressure drop rates, and water-cut decline rates were analyzed for different wettability indices in the Chang 7 reservoirs of the Ordos Basin. Results showed a consistent pattern: neutral wettability > weak oil-wet > oil-wet (Figs. 19, 20.).

The relationship between PFSID and fracturing parameters

As indicated in the previous evaluation of reservoir wettability, the overall wettability of the shale oil reservoirs in Longdong region exhibit a mixed characteristic, with a greater prevalence of oil-wet pores in Huachi area compared to Heshui area. This suggests that Heshui area is more favorable for fracturing fluid imbibition displacement. Numerical simulations have shown a nonlinear positive correlation between PFSID and the average volume of injected fluid for a single stage (Fig. 21). By considering both the injected fluid and reservoir parameters, the PFSID for Heshui and Huachi regions were optimized (Table 5).

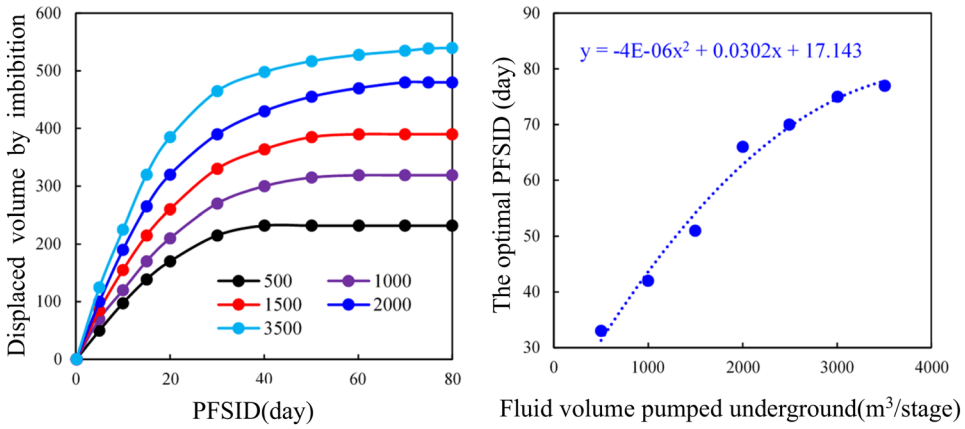

Fig. 21 Numerical simulation of the relationship between PFSID and injection volume

Table 5 Optimization of shut-in time for Huachi and Heshui areas

Area	Volume of injected fluid of each well (m^3)	Number of stages of each well	Matrix permeability (mD)	Porosity (%)	Oil saturation (%)	The optimal PFSID (day)
Huachi	29,188	37	0.13	8.8	55.6	36
Heshui	28,291	26	0.13	9.7	46.7	43

Conclusions

1. This study provided a quantitative way to estimate reservoir wettability in shale oil formation, and determines post-fracture shut-in duration (PFSID) of a horizontal well based on the wettability and fracturing parameters. It showed that shale oil reservoirs in the Longdong region generally exhibit mixed wettability, with large pores being predominantly water-wet and small pores being mainly oil-wet.
2. Combining the Amott method with nuclear magnetic resonance (NMR), we calculated the volume of water and oil both by imbibition and flooding at every step of NMR experiment in four samples from Longdong region in Ordos basin. With the fixed equation for wettability index calculation, the study gave both quantitative oil and water wettability in every pore throat scale and found that Huachi and Heshui areas in Longdong region show a slight different wettabilty, and this leads to a difference in the PFSID in two areas.
3. Four samples from Longdong region showed that because of the difference in wettability among large, medium, and small pores, large pores are the space where crude oil are developed from at the first stage of production. Then, recovery rate in the medium and small pores, especially the small pores, increases rapidly with the production goes by.
4. Quantitative reservoir wettability and fracturing parameters of a horizontal well are the two most decisive factors that affect PFSID. Numerical simulations have shown a nonlinear positive correlation between PFSID and the average volume of injected fluid and the optimal PFSID in Huachi and Heshui areas are determined to be 36 and 43 days, respectively.

Appendix

Method	Oil wet	Neutral wet	Water wet
A: Wettability Standards of contact angle and Amott methods			
Amott index	− 1.0 to − 0.3	− 0.3 to 0.3	0.3–1.0
Contact angle (°)			
Max	105–120	60–75	0
Min	180	105–120	60–75

Relaxation time	Signal amplitude				
	Bound water	After water imbibition	After water-flooding	After oil-imbibition	After oil-flooding
B (a): NMR logs for sample 1					
0.01	0	0	0	0	0
0.010719	0	0	0	0	0
0.01149	0.000001054	0.000001	0.000001	0.000001	0.000001
0.012316	0.000002108	0.000002	0.000006	0.000004	0.000004
0.013201	0.000009486	0.000009	0.000021	0.000015	0.000015
0.01415	0.000032674	0.000031	0.000073	0.000051	0.000051
0.015167	0.000102238	0.000097	0.000227	0.00016	0.00016
0.016258	0.000296174	0.000281	0.000657	0.000464	0.000464
0.017426	0.000797878	0.000757	0.001767	0.001249	0.001249
0.018679	0.001969926	0.001869	0.004366	0.003086	0.003085
0.020022	0.004582792	0.004348	0.010155	0.007177	0.007176
0.021461	0.010073078	0.009557	0.022321	0.015775	0.015772
0.023004	0.020680534	0.019621	0.045827	0.032387	0.032381
0.024658	0.040475708	0.038402	0.089689	0.063386	0.063374
0.026431	0.075732008	0.071852	0.167805	0.118595	0.118572
0.028331	0.135831088	0.128872	0.300954	0.212702	0.212661
0.030368	0.231496344	0.219636	0.512861	0.362485	0.362415
0.032551	0.37666798	0.35737	0.834335	0.589742	0.589626
0.034891	0.59930967	0.568605	1.327135	0.938182	0.937991
0.037399	0.906962784	0.860496	2.007572	1.419453	1.419148
0.040088	1.395226176	1.323744	3.086404	2.182827	2.182324
0.04297	2.12041085	2.011775	4.686318	3.315638	3.314799
0.046059	3.105648944	2.946536	6.854995	4.85266	4.851278
0.04937	4.432047866	4.204979	9.765565	6.918225	6.915957
0.05292	6.226682072	5.907668	13.687828	9.706535	9.702806
0.056724	8.481724558	8.047177	18.588415	13.198789	13.192765
0.060802	11.3170225	10.737213	24.706646	17.571924	17.562329
0.065173	14.93440004	14.16926	32.447748	23.124764	23.109637
0.069859	19.20373349	18.219861	41.480293	29.635697	29.612553
0.074881	24.4856458	23.231163	52.52057	37.635181	37.600357
0.080264	30.50553518	28.942633	64.897282	46.666671	46.616051
0.086035	37.47695047	35.556879	78.974222	57.018468	56.946908
0.09222	45.79494666	43.448716	95.464096	69.240371	69.141324
0.09885	54.8643363	52.05345	112.989225	82.373072	82.240967
0.105956	65.48368247	62.128731	133.055158	97.553908	97.381624
0.113573	76.7670887	72.83405	153.697015	113.389024	113.17273
0.121738	89.12432067	84.558179	175.605441	130.422588	130.159451
0.13049	103.2724188	97.981422	200.014724	149.619733	149.307755
0.139871	117.7928508	111.757923	223.998616	168.838514	168.484079

Relaxation time	Signal amplitude				
	Bound water	After water imbibition	After water-flooding	After oil-imbibition	After oil-flooding
0.149927	133.2867731	126.458039	248.602472	188.886792	188.499697
0.160705	150.7315903	143.009099	275.479075	211.061344	210.654907
0.172259	168.0786775	159.467436	300.723205	232.406706	232.00707
0.184642	187.4495059	177.845831	328.050849	255.803745	255.439579
0.197917	206.3284819	195.757573	352.921061	277.738287	277.451664
0.212145	225.7768362	214.209522	377.174476	299.63254	299.470627
0.227397	247.3092699	234.638776	403.229564	323.424543	323.441986
0.243744	267.7001257	253.984939	425.729129	344.829522	345.08885
0.261268	288.3503087	273.577143	447.011782	365.68728	366.255399
0.28005	311.1262685	295.186213	469.899976	388.311111	389.265059
0.300184	332.0964059	315.081979	488.397943	407.747343	409.157408
0.321764	355.2313623	337.031653	508.447489	428.90646	430.859604
0.344896	376.1285607	356.858217	523.713526	446.440307	449.001974
0.369691	396.804572	376.474926	537.239369	462.852753	466.094723
0.396269	419.7091177	398.205994	552.32974	480.98311	484.997104
0.424757	439.8034243	417.270801	562.35162	495.0459	499.874041
0.455294	459.457514	435.917945	570.625633	507.859161	513.55622
0.488025	481.4300212	456.764726	580.592755	522.474085	529.125268
0.52311	500.1165327	474.493864	585.516432	532.816467	540.424817
0.560717	521.2056645	494.502528	592.279782	545.069598	553.711474
0.601028	538.7377171	511.136354	594.144426	553.019461	562.666325
0.644236	555.6098361	527.144057	594.645458	559.83635	570.493263
0.690551	575.013233	545.553352	597.240736	568.762748	580.489631
0.740196	590.5581109	560.301813	595.339055	573.508731	586.229223
0.79341	605.3909296	574.374696	592.45483	577.336601	591.025868
0.850449	622.890656	590.977852	591.944129	583.504014	598.209575
0.911589	636.3194466	603.71864	587.453972	585.735984	601.343774
0.977124	652.5107511	619.080409	585.528225	590.471228	607.027758
1.047371	664.5132741	630.468002	579.978023	591.457249	608.834137
1.122668	675.7869435	641.164083	574.127161	591.966725	610.121646
1.203378	689.926773	654.579481	571.073459	595.185318	614.17844
1.28989	699.7607658	663.909645	564.919834	594.960982	614.662854
1.382622	708.8648321	672.547279	558.80725	594.501286	614.885653
1.482021	720.8976344	683.9636	555.646641	596.904924	618.060865
1.588565	728.5404097	691.21481	549.815439	596.138937	617.950873
1.702769	739.1407396	701.272049	546.990079	598.312918	620.890227
1.825183	749.0256291	710.650502	544.400502	600.442267	623.792002
1.956398	761.9735353	722.935043	544.791143	605.577095	629.82946
2.097046	774.2675273	734.599172	545.448057	610.754622	635.926306
2.247806	785.8897144	745.625915	546.374586	615.994823	642.098107
2.409404	796.8269807	756.002828	547.555776	621.3081	648.346802
2.582619	807.0724436	765.723381	548.958067	626.694568	654.659992
2.768287	816.6268218	774.788256	550.529333	632.143459	661.010616
2.967302	825.4996194	783.20647	552.199318	637.632681	667.35701
3.180626	833.7100011	790.996206	553.880505	643.128614	673.643369
3.409285	841.2872725	798.185268	555.469486	648.586184	679.800612
3.654383	848.2708994	804.8111	556.848866	653.949266	685.747621
3.917101	854.7100268	810.920329	557.889759	659.151439	691.392859
4.198707	860.6624897	816.567827	558.454866	664.117093	696.636306
4.500558	866.1933504	821.815323	558.402124	668.762866	701.371712

Relaxation time	Signal amplitude				
	Bound water	After water imbibition	After water-flooding	After oil-imbibition	After oil-flooding
4.824109	871.3730269	826.729627	557.588817	672.99936	705.489082
5.17092	876.2751134	831.380563	555.876043	676.733083	708.877345
5.542665	880.9739951	835.838705	553.133323	679.868494	711.427115
5.941134	885.5423768	840.173033	549.243154	682.310095	713.033464
6.36825	890.0488623	844.448636	544.105245	683.964429	713.598579
6.826072	894.5556683	848.724543	537.640217	684.741913	713.034218
7.316807	899.1165877	853.051791	529.792546	684.558413	711.263868
7.842822	903.7752624	857.471786	520.532606	683.336517	708.2245
8.406653	908.5638163	862.015006	509.857687	681.006481	703.867895
9.011018	913.5018706	866.700067	497.791998	677.506873	698.161472
9.658832	918.5959538	871.533163	484.385663	672.784943	691.088652
10.353218	923.8392918	876.507867	469.712846	666.796811	682.648745
11.097525	929.2119472	881.605263	453.869136	659.507559	672.856449
11.895341	934.6812955	886.794398	436.968396	650.891301	661.741002
12.750512	940.2027746	892.032993	419.13927	640.931336	649.345085
13.667164	945.7208936	897.2684	400.521532	629.620429	635.72355
14.649714	951.1704393	902.438747	381.262461	616.961251	620.942047
15.702901	956.4778521	907.474243	361.513386	602.966973	605.07561
16.831804	961.5627297	912.298605	341.42648	587.661979	588.207242
18.041864	966.3394197	916.830569	321.151901	571.082611	570.426495
19.338918	970.7186843	920.985469	300.835278	553.277876	551.82807
20.729218	974.6093841	924.676835	280.615572	534.310008	532.510379
22.219469	977.9201678	927.817996	260.623263	514.254799	512.574089
23.816856	980.5611218	930.323645	240.978865	493.201628	492.120603
25.529081	982.4453492	932.111337	221.791712	471.253158	471.250502
27.3644	983.490426	933.102871	203.159	448.524674	450.061975
29.331663	983.6197023	933.225524	185.165047	425.143104	428.649288
31.440355	982.7633937	932.413087	167.880768	401.245757	407.101374
33.700643	980.8594376	930.606677	151.363326	376.978858	385.500635
36.123427	977.8540841	927.755298	135.65596	352.495932	363.92203
38.720388	973.7022179	923.816146	120.787964	327.956139	342.432537
41.504048	968.367418	918.754666	106.77481	303.522594	321.091013
44.487828	961.8217786	912.544382	93.618386	279.360721	299.948458
47.686117	954.0455511	905.166557	81.307352	255.636683	279.048643
51.114335	945.0266249	896.609701	69.817607	232.515877	258.429012
54.789012	934.7599281	886.869002	59.112875	210.161486	238.121754
58.727866	923.2467899	875.945721	49.145431	188.73308	218.154913
62.94989	910.4942879	863.846573	39.857008	168.385209	198.553402
67.475441	896.5146232	850.583134	31.179916	149.265961	179.339817
72.326339	881.3245154	836.171267	23.038418	131.515421	160.53495
77.525975	864.9446155	820.630565	25.824167	115.263989	142.157965
83.099419	847.3988925	803.983769	28.706515	100.630481	124.226206
89.073546	828.7139895	786.256157	31.47075	87.719991	106.754669
95.477161	808.9184993	767.474857	34.038068	76.621475	89.755197
102.34114	788.0421658	747.668089	36.327792	67.405076	73.235459
109.69858	766.1150144	726.86434	38.267445	60.119245	57.197831
117.584955	743.1664747	705.091532	39.798141	54.787776	41.638263
126.038293	719.2245643	682.376247	40.877675	51.406919	26.545269
135.099352	694.3152411	658.743113	41.487626	49.942801	21.147802
144.811823	668.4620282	634.214448	41.682174	50.3294	22.844088

Relaxation time	Signal amplitude				
	Bound water	After water imbibition	After water-flooding	After oil-imbibition	After oil-flooding
155.222536	641.6860183	608.810264	41.468216	52.467337	24.63775
166.381689	614.0063119	582.548683	40.810964	56.22373	26.541698
178.343088	585.440924	555.446797	39.689835	61.433285	28.459872
191.164408	556.0081026	527.521919	38.116077	67.900732	30.310761
204.907469	525.7279896	498.793159	36.112931	75.404617	32.012972
219.638537	494.624477	469.283185	33.713439	83.702334	33.488145
235.428641	462.7270958	439.020015	30.958839	92.53621	34.660939
252.353917	430.072775	408.038686	27.895282	101.640333	35.461139
270.495973	396.7072931	376.382631	24.576405	110.747792	35.824403
289.942285	362.686319	344.104667	21.042399	119.597945	35.694363
310.786619	328.0759302	311.267486	17.3389	127.943344	35.023752
333.129479	292.9525839	277.943628	13.513303	135.555986	33.774734
357.078596	257.4025362	244.21493	9.609675	142.232622	31.920925
382.749448	221.5207821	210.17152	5.668133	147.798913	29.451362
410.265811	185.4095616	175.9104	1.723831	152.112331	26.354974
439.760361	149.1765767	141.533754	1.417996	155.063776	22.638522
471.375313	112.932997	107.147056	1.241222	156.577945	18.318967
505.263107	76.79138656	72.857103	1.0874	156.612567	13.422528
541.587138	40.8636601	38.770076	0.955767	155.156664	7.983718
580.522552	6.262581312	5.941728	0.844899	152.228009	3.977463
622.257084	6.263002912	5.942128	0.752875	147.869988	2.376889
666.991966	6.176242902	5.859813	0.677436	142.148066	0.543982
714.942899	6.013308204	5.705226	0.616155	135.146037	0
766.341087	5.78556937	5.489155	0.566562	126.962228	0
821.434358	5.504252554	5.222251	0.526264	117.705794	0
880.488358	5.180076936	4.914684	0.493023	107.493226	0
943.787828	4.82300914	4.57591	0.464817	96.445144	0
1011.63798	4.442110404	4.214526	0.439876	84.683439	0
1084.365969	4.045443828	3.838182	0.416702	72.328801	0
1162.322469	3.640060672	3.453568	0.394065	59.498634	0
1245.883364	3.232003518	3.066417	0.370994	46.305366	0
1335.451563	2.826357916	2.681554	0.346766	33.630931	0
1431.458938	2.427318786	2.302959	0.320871	22.800467	0
1534.368409	2.038269468	1.933842	0.292996	12.087011	0
1644.676178	1.661877636	1.576734	0.262991	1.543704	0
1762.914118	1.30017751	1.233565	0.230849	0	0
1889.65234	0.954673148	0.905762	0.196676	0	0
2025.501939	0.626425928	0.594332	0.160675	0	0
2171.117946	0.316148354	0.299951	0.123128	0	0
2327.202479	0.0242947	0.02305	0.084386	0	0
2494.508135	0	0	0.044863	0	0
2673.841616	0	0	0.005045	0	0
2866.067617	0	0	0	0	0
3072.112999	0	0	0	0	0
3292.971255	0	0	0.01094	0	0
3529.707303	0	0	0.048491	0	0
3783.462617	0	0	0.09525	0	0
4055.460736	0	0	0.144169	0	0
4347.013158	0	0	0.192895	0	0
4659.525669	0	0	0.240381	0	0

Relaxation time	Signal amplitude				
	Bound water	After water imbibition	After water-flooding	After oil-imbibition	After oil-flooding
4994.505116	0	0	0.286118	0	0
5353.566677	0.008839898	0.008387	0.514957	0	0
5738.441648	0.516910058	0.490427	0.935206	0	0
6150.985789	1.009121734	0.957421	1.345001	0	0
6593.188271	1.482971676	1.406994	1.739303	0	0
7067.181274	1.937263594	1.838011	2.117209	0	0
7575.250259	2.371469434	2.249971	2.478406	0	0
8119.844993	2.785481688	2.642772	2.82019	0	0
8703.591361	3.179478482	3.016583	3.143113	0	0
9329.304026	3.553770746	3.371699	3.447856	0	0
10,000	3.908868616	3.708604	3.735149	0	0
Relaxtion time	Signal amplitude				
	Bound water	After water imbibition	After water-flooding	After oil-imbibition	After oil-flooding
B (b): NMR logs for sample 2					
0.01	0	0	0	0	0
0.010719	0	0	0	0	0
0.01149	0	0	0.000001	0.000001	0.000001
0.012316	0.000002	0.000002	0.000004	0.000004	0.000003
0.013201	0.000007	0.000007	0.000015	0.000013	0.000012
0.01415	0.000023	0.000024	0.00005	0.000045	0.00004
0.015167	0.000071	0.000074	0.000155	0.000139	0.000124
0.016258	0.000205	0.000214	0.000447	0.000403	0.00036
0.017426	0.000551	0.000576	0.001204	0.001086	0.000968
0.018679	0.001361	0.001423	0.002974	0.002682	0.002392
0.020022	0.003166	0.00331	0.006919	0.006238	0.005563
0.021461	0.006959	0.007275	0.015207	0.013711	0.012226
0.023004	0.014288	0.014937	0.03122	0.028149	0.025101
0.024658	0.027964	0.029234	0.061103	0.055092	0.049127
0.026431	0.052322	0.054697	0.114321	0.103075	0.091915
0.028331	0.093845	0.098099	0.20503	0.184862	0.164849
0.030368	0.159943	0.167179	0.349393	0.315027	0.280926
0.032551	0.260252	0.271987	0.568392	0.512491	0.457027
0.034891	0.414106	0.432679	0.904091	0.815189	0.726995
0.037399	0.626741	0.654619	1.367576	1.233132	1.099791
0.040088	0.964273	1.006631	2.102369	1.895764	1.690934
0.04297	1.465741	1.528953	3.191926	2.878415	2.567769
0.046059	2.147362	2.237557	4.668511	4.210317	3.756663
0.04937	3.065598	3.189666	6.649676	5.997718	5.352905
0.05292	4.309013	4.474649	9.318508	8.406168	7.5051
0.056724	5.873253	6.083593	12.651292	11.414931	10.196087
0.060802	7.842852	8.097755	16.809449	15.170632	13.558789
0.065173	10.360035	10.654484	22.066446	19.921585	17.818112
0.069859	13.337812	13.651354	28.193764	25.463631	22.795553
0.074881	17.030915	17.332612	35.674153	32.235644	28.889296
0.080264	21.254008	21.488294	44.046131	39.824561	35.736125
0.086035	26.162206	26.252276	53.550344	48.45258	43.543099
0.09222	32.039735	31.879956	64.661552	58.555682	52.712209
0.09885	38.479943	37.933592	76.436516	69.287549	62.493234

Relaxtion time	Signal amplitude				
	Bound water	After water imbibition	After water-flooding	After oil-imbibition	After oil-flooding
0.105956	46.052945	44.943115	89.882976	81.570422	73.729726
0.113573	54.147583	52.275347	103.660398	94.198778	85.34593
0.121738	63.062266	60.192623	118.223289	107.595837	97.735839
0.13049	73.316938	69.156149	134.386931	122.517772	111.600951
0.139871	83.916736	78.195336	150.168779	137.17262	125.323235
0.149927	95.2958	87.70442	166.25917	152.202366	139.495541
0.160705	108.16301	98.312072	183.746563	168.620717	155.059295
0.172259	121.056605	108.671071	200.009822	184.039759	169.829452
0.184642	135.505855	120.156027	217.511543	200.737158	185.910178
0.197917	149.69618	131.149678	233.227216	215.937883	200.73854
0.212145	164.389045	142.344864	248.37636	230.772501	215.356478
0.227397	180.686473	154.696602	264.542816	246.725096	231.152038
0.243744	196.228777	166.189002	278.206423	260.522299	245.059644
0.261268	212.026373	177.717843	290.913925	273.599308	258.410539
0.28005	229.445521	190.437832	304.504234	287.688393	272.838807
0.300184	245.579858	201.947842	315.0982	299.123549	284.864472
0.321764	263.350707	214.68408	326.55601	311.547673	297.938892
0.344896	279.487531	225.993276	334.823588	321.084122	308.350208
0.369691	295.471746	237.118961	341.893178	329.600936	317.864269
0.396269	313.123289	249.535154	349.890535	339.131741	328.437582
0.424757	328.680653	260.257933	354.639929	345.610907	336.128224
0.455294	343.905	270.724685	358.293118	351.081745	342.894114
0.488025	360.86305	282.576858	363.042692	357.671324	350.808751
0.52311	375.357845	292.543224	364.710461	361.241625	355.809649
0.560717	391.659136	303.983797	367.636701	366.047973	362.066879
0.601028	405.295814	313.445845	367.67563	367.943066	365.473925
0.644236	418.448116	322.653143	367.071252	369.123597	368.181503
0.690551	433.528601	333.486516	367.995007	371.759542	372.348285
0.740196	445.729088	342.269504	366.421529	371.774831	373.885034
0.79341	457.425714	350.860189	364.55472	371.373714	374.975371
0.850449	471.180171	361.248475	364.49143	372.692589	377.768037
0.911589	481.903254	369.558399	362.348485	371.766583	378.235385
0.977124	494.770599	379.785739	362.182572	372.7543	380.583907
1.047371	504.516029	387.914205	360.186742	371.754017	380.82198
1.122668	513.759137	395.972749	358.418883	370.893874	381.102879
1.203378	525.23392	406.091805	358.825629	372.213898	383.518421
1.28989	533.479241	414.069588	357.710074	371.908565	384.145956
1.382622	541.206235	422.00284	357.022013	372.024042	385.086059
1.482021	551.202617	432.078264	358.621916	374.533848	388.387198
1.588565	557.864513	439.911321	358.878221	375.681911	390.164028
1.702769	566.799735	449.9027	361.450697	379.328619	394.432919
1.825183	575.183207	459.824147	364.52464	383.613823	399.27916
1.956398	585.901402	471.980799	369.931429	390.506691	406.772205
2.097046	596.082666	484.071217	375.846757	398.131759	414.982944
2.247806	605.69006	496.037631	382.237498	406.494617	423.941409
2.409404	614.689202	507.818791	389.053959	415.584765	433.663202
2.582619	623.050424	519.352809	396.229581	425.375284	444.148194
2.768287	630.751191	530.580329	403.680904	435.822667	455.379359
2.967302	637.778676	541.447843	411.3079	446.866804	467.32178

Relaxtion time	Signal amplitude				
	Bound water	After water imbibition	After water-flooding	After oil-imbibition	After oil-flooding
3.180626	644.132378	551.910919	418.994772	458.431134	479.921905
3.409285	649.826614	561.937116	426.611311	470.422995	493.1071
3.654383	654.892694	571.508365	434.014885	482.734236	506.785607
3.917101	659.380594	580.622634	441.05308	495.242151	520.846982
4.198707	663.359922	589.294732	447.566988	507.810816	535.163086
4.500558	666.920015	597.556199	453.395051	520.292857	549.589694
4.824109	670.169044	605.45428	458.377353	532.53169	563.96872
5.17092	673.232065	613.050065	462.360176	544.364201	578.131041
5.542665	676.24804	620.415917	465.200614	555.623817	591.899824
5.941134	679.365914	627.63239	466.771031	566.14385	605.094251
6.36825	682.739936	634.784805	466.963128	575.76099	617.533453
6.826072	686.524436	641.959711	465.69142	584.318806	629.040511
7.316807	690.868336	649.2414	462.895942	591.671076	639.446316
7.842822	695.909681	656.708638	458.544068	597.684822	648.59313
8.406653	701.770451	664.431729	452.631354	602.242915	656.337725
9.011018	708.551905	672.470001	445.181392	605.246155	662.553978
9.658832	716.330645	680.869754	436.244727	606.614775	667.134882
10.353218	725.15553	689.6627	425.896905	606.289343	669.993933
11.097525	735.045518	698.864867	414.235808	604.231074	671.065935
11.895341	745.988449	708.475964	401.378426	600.421609	670.307232
12.750512	757.940739	718.479161	387.457239	594.862322	667.695462
13.667164	770.827908	728.841239	372.616412	587.573253	663.228882
14.649714	784.545861	739.513068	357.007936	578.591779	656.925361
15.702901	798.962794	750.430388	340.787902	567.971098	648.821111
16.831804	813.921639	761.514843	324.113006	555.77867	638.969241
18.041864	829.242928	772.675259	307.137394	542.094651	627.438197
19.338918	844.727998	783.809141	290.009899	527.010434	614.310149
20.729218	860.162464	794.804378	272.87172	510.627299	599.679378
22.219469	875.319918	805.541138	255.854529	493.055218	583.650674
23.816856	889.96581	815.893931	239.079019	474.411782	566.33779
25.529081	903.861497	825.733814	222.653824	454.821225	547.861923
27.3644	916.768436	834.930681	206.674794	434.413491	528.350248
29.331663	928.452513	843.355605	191.224539	413.323275	507.934454
31.440355	938.688452	850.883145	176.3722	391.688984	486.749296
33.700643	947.264285	857.393562	162.173399	369.651555	464.931138
36.123427	953.985793	862.774855	148.670298	347.353105	442.616469
38.720388	958.680841	866.924549	135.891781	324.93539	419.940412
41.504048	961.203485	869.751161	123.853728	302.538095	397.035213
44.487828	961.437741	871.175295	112.559393	280.296984	374.028727
47.686117	959.300884	871.130316	101.999929	258.341962	351.042916
51.114335	954.746145	869.562606	92.155059	236.795115	328.192381
54.789012	947.764702	866.431384	82.993929	215.768791	305.582932
58.727866	938.386863	861.708147	74.476145	195.363781	283.310245
62.94989	926.682364	855.375768	66.552976	175.667672	261.458603
67.475441	912.759726	847.427341	59.168706	156.753396	240.099788
72.326339	896.764628	837.864849	52.262102	138.678048	219.292146
77.525975	878.87726	826.697776	45.767951	121.481986	199.079898
83.099419	859.308656	813.941745	39.618642	105.188269	179.492734
89.073546	838.295991	799.617314	33.745778	89.802462	160.545776

Relaxtion time	Signal amplitude				
	Bound water	After water imbibition	After water-flooding	After oil-imbibition	After oil-flooding
95.477161	816.096885	783.749001	28.081789	75.312835	142.239937
102.34114	792.982771	766.364623	22.561544	61.690978	124.562724
109.69858	769.231455	747.494987	23.982652	48.892823	107.489471
117.584955	745.119063	727.173933	25.949247	36.860051	90.984992
126.038293	720.911632	705.438707	27.644731	25.521827	75.005556
135.099352	696.856695	682.330579	29.040762	14.796794	59.501099
144.811823	673.175264	657.895622	30.122767	5.361726	44.417524
155.222536	650.054635	632.185523	30.925479	9.465515	29.698957
166.381689	627.64246	605.258332	31.469921	13.621779	15.289822
178.343088	606.042461	577.179027	31.735001	17.808839	9.741187
191.164408	585.312104	548.019838	31.711639	21.907727	12.675915
204.907469	565.462388	517.860282	31.40717	25.780106	15.499292
219.638537	546.459796	486.786889	30.826847	29.310554	18.143498
235.428641	528.230283	454.892652	29.975698	32.395907	20.552498
252.353917	510.665019	422.276231	28.873698	34.944775	22.680549
270.495973	493.627529	389.040959	27.543184	36.877952	24.490841
289.942285	476.961733	355.29373	26.007245	38.128158	25.954729
310.786619	460.50041	321.143798	24.287656	38.640514	27.049916
333.129479	444.073569	286.701566	22.405299	38.372913	27.760608
357.078596	427.516292	252.077384	20.377928	37.295819	28.076507
382.749448	410.675665	217.380402	18.22169	35.39212	27.99184
410.265811	393.416529	182.7175	15.949616	32.657539	27.506128
439.760361	375.625872	148.192306	13.573111	29.099849	26.622676
471.375313	357.215807	113.904313	11.105764	24.738387	25.349242
505.263107	338.125154	79.948108	8.551626	19.602678	23.697361
541.587138	318.319728	46.412704	5.917216	13.731729	21.68236
580.522552	297.791501	13.380985	3.209969	7.173163	19.322692
622.257084	276.556829	2.348625	0.437214	0	16.639801
666.991966	254.653966	2.573518	0	0	13.657812
714.942899	232.140071	2.761963	0.062754	0	10.402968
766.341087	209.087924	2.912451	0.272089	0	6.903187
821.434358	185.582524	3.024484	0.476111	0	3.187766
880.488358	161.717731	3.098407	0.668896	0	0
943.787828	137.593069	3.135254	0.845665	0	0
1011.63798	113.310792	3.136626	1.002748	0	0
1084.365969	88.973266	3.104575	1.137517	0	0
1162.322469	64.680714	3.041495	1.248291	0	0
1245.883364	40.52934	2.95003	1.33423	0	0
1335.451563	33.608527	2.832988	1.39522	0	0
1431.458938	28.761475	2.693262	1.431756	0	0
1534.368409	23.762565	2.53377	1.444833	0	0
1644.676178	18.670145	2.3574	1.435836	0	0
1762.914118	13.503184	2.166965	1.406449	0	0
1889.65234	8.273776	1.965179	1.358574	0	0
2025.501939	3.000212	1.754632	1.294262	0	0
2171.117946	0	1.537787	1.215669	0	0
2327.202479	0	1.316991	1.12502	0	0
2494.508135	0	1.094499	1.024613	0	0
2673.841616	0	0.872541	0.91685	0	0

Relaxtion time	Signal amplitude				
	Bound water	After water imbibition	After water-flooding	After oil-imbibition	After oil-flooding
2866.067617	0	0.653427	0.804327	0	0
3072.112999	0	0.439771	0.690027	0	0
3292.971255	0	0.234933	0.577646	0	0
3529.707303	0	0.044001	0.471959	0	0
3783.462617	0	0	0.390245	0	0
4055.460736	0	0	0.335498	0	0
4347.013158	0	0	0.29659	0	0
4659.525669	0	0	0.265218	0	0
4994.505116	0	0.087856	0.236068	0	0
5353.566677	0	0.400683	0.206591	0	0
5738.441648	0	0.739764	0.175942	0	0
6150.985789	0	1.090314	0.144042	0	0
6593.188271	0	1.426675	0.111084	0	0
7067.181274	0	1.747181	0.077348	0	0
7575.250259	0	2.051376	0.043138	0	0
8119.844993	0	2.339354	0.008735	0	0
8703.591361	0	2.611474	0.002461	0	0
9329.304026	0	2.868256	0.000267	0	0
10,000	0	3.110304	0	0	0
Relaxtion time	Signal amplitude				
	Bound water	After water imbibition	After water-flooding	After oil-imbibition	After oil-flooding
B (c): NMR logs for sample 3					
0.01	0	0	0	0	0
0.010719	0	0	0	0	0
0.01149	0	0	0.000001	0.000001	0
0.012316	0.00000242	0.000002	0.000003	0.000002	0.000002
0.013201	0.00000726	0.000006	0.00001	0.000008	0.000007
0.01415	0.00002299	0.000019	0.000034	0.000026	0.000023
0.015167	0.00007139	0.000059	0.000106	0.000082	0.000071
0.016258	0.00020449	0.000169	0.000306	0.000238	0.000206
0.017426	0.00055176	0.000456	0.000824	0.000641	0.000554
0.018679	0.00136246	0.001126	0.002036	0.001585	0.001368
0.020022	0.00316778	0.002618	0.004735	0.003686	0.003183
0.021461	0.00696355	0.005755	0.010407	0.008101	0.006995
0.023004	0.01429615	0.011815	0.021367	0.016633	0.014361
0.024658	0.02798004	0.023124	0.041819	0.032553	0.028108
0.026431	0.05234944	0.043264	0.078243	0.060906	0.05259
0.028331	0.09389358	0.077598	0.140329	0.109237	0.094323
0.030368	0.16002129	0.132249	0.239145	0.186165	0.160751
0.032551	0.26036659	0.215179	0.389066	0.302891	0.26155
0.034891	0.4142556	0.34236	0.618916	0.481878	0.416129
0.037399	0.62689132	0.518092	0.936356	0.729139	0.629703
0.040088	0.96432765	0.796965	1.439799	1.121417	0.968602
0.04297	1.46543947	1.211107	2.186733	1.703727	1.471818
0.046059	2.14612497	1.773657	3.199869	2.494204	2.155225
0.04937	3.0622801	2.53081	4.560814	3.557207	3.074792
0.05292	4.30144231	3.554911	6.396929	4.993375	4.318124

Relaxtion time	Signal amplitude				
	Bound water	After water imbibition	After water-flooding	After oil-imbibition	After oil-flooding
0.056724	5.85777819	4.841139	8.694755	6.79426	5.878897
0.060802	7.81343585	6.457385	11.569281	9.052697	7.838859
0.065173	10.30679452	8.518012	15.214822	11.925247	10.335741
0.069859	13.24668796	10.947676	19.482132	15.301152	13.276551
0.074881	16.88006265	13.950465	24.715345	19.458698	16.906644
0.080264	21.01515174	17.367894	30.608407	24.167445	21.030959
0.086035	25.7962078	21.31918	37.34315	29.582526	25.790249
0.09222	31.49123131	26.025811	45.269653	35.996611	31.447361
0.09885	37.68619899	31.145619	53.748606	42.918917	37.582463
0.105956	44.92444561	37.127641	63.50881	50.949225	44.730008
0.113573	52.5917788	43.46428	73.626276	59.367514	52.268972
0.121738	60.96311782	50.382742	84.439359	68.4632	60.463201
0.13049	70.52102398	58.281838	96.552262	78.749339	69.778244
0.139871	80.28841139	66.354059	108.560534	89.103774	79.232423
0.149927	90.66907036	74.933116	120.967722	99.952162	89.21149
0.160705	102.3189976	84.561155	134.580101	111.983175	100.342324
0.172259	113.8388364	94.081683	147.488827	123.629871	111.23236
0.184642	126.6599045	104.677607	161.505828	136.42102	123.262585
0.197917	139.0748251	114.937872	174.389413	148.481583	134.748155
0.212145	151.7986418	125.453423	187.029309	160.563577	146.368492
0.227397	165.8444319	137.061514	200.616085	173.703698	159.075053
0.243744	179.0453202	147.971339	212.475624	185.598869	170.763518
0.261268	192.3448622	158.962696	223.754613	197.230486	182.325444
0.28005	206.9880801	171.064529	235.859111	209.845281	194.915064
0.300184	220.3615313	182.116968	245.774958	220.766167	206.046118
0.321764	235.1109896	194.306603	256.482476	232.647828	218.184193
0.344896	248.3296141	205.231086	264.786984	242.591421	228.608987
0.369691	261.3691125	216.007531	272.220614	251.953173	238.576578
0.396269	275.8552228	227.979523	280.465862	262.283476	249.552311
0.424757	288.4908439	238.422185	286.166184	270.433732	258.537469
0.455294	300.8574952	248.642558	291.015712	277.94268	266.978505
0.488025	314.7809071	260.14951	296.788107	286.489555	276.485397
0.52311	326.6179947	269.932227	300.061814	292.754633	283.851332
0.560717	340.1117961	281.084129	304.381	300.141466	292.358358
0.601028	351.3979162	290.411501	306.310546	305.24275	298.684318
0.644236	362.3943357	299.499451	307.686387	309.812294	304.51884
0.690551	375.2091529	310.090209	310.329923	315.662736	311.639697
0.740196	385.7000308	318.760356	310.850024	319.323412	316.616041
0.79341	395.9436705	327.226174	311.09113	322.615961	321.226484
0.850449	408.1775159	337.33679	312.851131	327.385265	327.30238
0.911589	418.0135587	345.465751	312.808265	330.13719	331.34437
0.977124	429.9581681	355.337329	314.458687	334.514049	336.987422
1.047371	439.4573759	363.187914	314.513784	337.004098	340.687198
1.122668	448.8000558	370.909137	314.760662	339.473	344.304275
1.203378	460.3989742	380.49502	316.929813	343.780732	349.719043
1.28989	469.4927183	388.010511	317.778043	346.407485	353.345593
1.382622	478.4653947	395.425946	319.031016	349.211277	357.060124
1.482021	489.8098949	404.801566	322.372793	354.045279	362.754565
1.588565	498.5761972	412.046444	324.55844	357.362634	366.793427

Relaxtion time	Signal amplitude				
	Bound water	After water imbibition	After water-flooding	After oil-imbibition	After oil-flooding
1.702769	509.7803193	421.306049	328.894417	362.818336	372.921384
1.825183	520.9313744	430.521797	333.751972	368.651636	379.332636
1.956398	534.6823407	441.886232	340.815571	376.763456	387.985072
2.097046	548.473634	453.283995	348.416995	385.361242	397.037199
2.247806	562.2917735	464.703945	356.51091	394.454352	406.501635
2.409404	576.1203129	476.13249	365.029715	404.038585	416.378908
2.582619	589.9395729	487.553366	373.883484	414.094865	426.655926
2.768287	603.7262935	498.94735	382.960612	424.588067	437.304582
2.967302	617.4532172	510.291915	392.129214	435.466044	448.280584
3.180626	631.0886636	521.560879	401.239292	446.658937	459.522606
3.409285	644.5961525	532.724093	410.125664	458.07889	470.951869
3.654383	657.9341495	543.747231	418.611598	469.620251	482.472247
3.917101	671.0560066	554.591741	426.513055	481.160362	493.970995
4.198707	683.9101911	565.215034	433.643401	492.561006	505.320149
4.500558	696.4408398	575.570942	439.818421	503.670531	516.378619
4.824109	708.5886905	585.610488	444.861429	514.32665	526.99495
5.17092	720.2923913	595.282968	448.608267	524.359825	537.010677
5.542665	731.4901451	604.53731	450.911974	533.59714	546.264147
5.941134	742.1216468	613.323675	451.646939	541.866495	554.594654
6.36825	752.1301799	621.59519	450.712357	549.000938	561.846711
6.826072	761.4647576	629.309717	448.03488	554.842943	567.874254
7.316807	770.0821525	636.431531	443.570368	559.248437	572.544601
7.842822	777.9486735	642.932788	437.304731	562.09042	575.741989
8.406653	785.0415229	648.794647	429.253865	563.262026	577.370542
9.011018	791.3496473	654.007973	419.462759	562.678951	577.356574
9.658832	796.8739786	658.573536	408.003864	560.281179	575.650152
10.353218	801.6270534	662.501697	394.974852	556.034017	572.225887
11.097525	805.6320179	665.811585	380.495873	549.928463	567.082974
11.895341	808.921081	668.529819	364.706476	541.98096	560.244506
12.750512	811.5335109	670.688852	347.762287	532.232616	551.756159
13.667164	813.5132972	672.325039	329.831561	520.747956	541.684323
14.649714	814.9065892	673.47652	311.091715	507.613281	530.113799
15.702901	815.7590572	674.181039	291.725893	492.934682	517.145189
16.831804	816.1132738	674.47378	271.919628	476.835767	502.892098
18.041864	816.0062215	674.385307	251.857648	459.455134	487.478278
19.338918	815.4670152	673.939682	231.72085	440.943642	471.034819
20.729218	814.5149195	673.152826	211.683456	421.461524	453.697495
22.219469	813.1577339	672.031185	191.910383	401.175409	435.604342
23.816856	811.390616	670.570757	172.554844	380.255322	416.89352
25.529081	809.1954098	668.756537	153.75618	358.871759	397.701501
27.3644	806.5405403	666.56243	135.637976	337.192901	378.161573
29.331663	803.3815013	663.951654	118.306467	315.382068	358.402662
31.440355	799.6619734	660.877664	101.849272	293.595456	338.548397
33.700643	795.3155264	657.285559	86.334505	271.9802	318.716391
36.123427	790.2678638	653.113937	71.810268	250.672794	299.017645
38.720388	784.4395079	648.297114	58.304597	229.797837	279.556014
41.504048	777.748796	642.7676	45.825845	209.467102	260.427675
44.487828	770.1150379	636.458709	34.363548	189.778883	241.720547
47.686117	761.4616987	629.307189	23.889743	170.817574	223.513645

Relaxtion time	Signal amplitude				
	Bound water	After water imbibition	After water-flooding	After oil-imbibition	After oil-flooding
51.114335	751.7194515	621.255745	14.360734	152.653441	205.876378
54.789012	740.8289832	612.255358	5.719245	135.342542	188.86782
58.727866	728.7434814	602.26734	0	118.926749	172.536005
62.94989	715.4307045	591.265045	2.256509	103.433852	156.917322
67.475441	700.8746174	579.235221	4.717321	88.877707	142.036058
72.326339	685.0765646	566.178979	7.266676	75.258422	127.904163
77.525975	668.0559411	552.112348	9.836499	62.562569	114.521264
83.099419	649.850344	537.0664	12.373121	50.763446	101.874947
89.073546	630.5151865	521.086931	14.80691	39.821391	89.941293
95.477161	610.1227298	504.233661	17.082421	29.684208	78.685643
102.34114	588.7605029	486.578928	19.154573	20.287734	68.063553
109.69858	566.5291233	468.205887	20.990894	11.556602	58.021865
117.584955	543.5395044	449.206202	22.572781	7.184142	48.499868
126.038293	519.9095221	429.677291	23.888205	11.320171	39.43047
135.099352	495.7602344	409.719202	24.937507	15.525989	30.741366
144.811823	471.2118173	389.431254	25.742839	19.703233	22.356157
155.222536	446.3794036	368.908598	26.299001	23.752808	19.666419
166.381689	421.3690835	348.238912	26.61775	27.581647	23.256696
178.343088	396.2743151	327.499434	26.725028	31.131758	26.754998
191.164408	371.1729874	306.754535	26.675411	34.351377	30.090653
204.907469	346.125363	286.054019	26.554537	37.086289	33.146453
219.638537	321.1730394	265.432264	26.302822	39.225717	35.816828
235.428641	296.3390019	244.908266	25.898407	40.680089	38.010858
252.353917	271.6287497	224.48657	25.334502	41.376309	39.647821
270.495973	247.0323973	204.159006	24.602596	41.257935	40.656268
289.942285	222.5275414	183.907059	23.692238	40.284559	40.97471
310.786619	198.0827052	163.704715	22.592857	38.431947	40.55176
333.129479	173.6610537	143.521532	21.270971	35.691559	39.350029
357.078596	149.2241406	123.325736	19.710388	32.069357	37.332936
382.749448	124.7354394	103.08714	17.894655	27.585072	34.481911
410.265811	100.1634515	82.779712	15.808402	22.270657	30.790237
439.760361	75.48425038	62.383678	13.438895	16.168967	26.263463
471.375313	50.6833668	41.88708	10.776133	9.33198	20.918292
505.263107	25.75696871	21.286751	7.814721	1.819191	14.781864
541.587138	24.88024022	20.562182	4.552957	0	7.892021
580.522552	24.80967181	20.503861	0.994501	0	0.294733
622.257084	24.25302704	20.043824	0.648555	0	0
666.991966	23.20167256	19.174936	0.591796	0	0
714.942899	21.65830667	17.899427	0.436898	0	0
766.341087	19.63581587	16.227947	0.178371	0	0
821.434358	17.15593297	14.178457	0	0	0
880.488358	14.24819044	11.775364	0	0	0
943.787828	10.94745443	9.047483	0	0	0
1011.63798	7.29372996	6.027876	0	0	0
1084.365969	3.77844643	3.122683	0	0	0
1162.322469	1.71424088	1.416728	0	0	0
1245.883364	0	0	0	0	0
1335.451563	0	0	0	0	0
1431.458938	0	0	0	0	0

Relaxtion time	Signal amplitude				
	Bound water	After water imbibition	After water-flooding	After oil-imbibition	After oil-flooding
1534.368409	0	0	0	0	0
1644.676178	0	0	0	0	0
1762.914118	0	0	0	0	0
1889.65234	0	0	0	0	0
2025.501939	0	0	0	0	0
2171.117946	0	0	0	0	0
2327.202479	0	0	0	0	0
2494.508135	0	0	0	0	0
2673.841616	0	0	0	0	0
2866.067617	0	0	0	0	0
3072.112999	0	0	0	0	0
3292.971255	0	0	0	0	0
3529.707303	0	0	0	0	0
3783.462617	0	0	0	0	0
4055.460736	0	0	0	0	0
4347.013158	0	0	0	0	0
4659.525669	0	0	0	0	0
4994.505116	0	0	0	0	0
5353.566677	0	0	0	0	0
5738.441648	0	0	0	0	0
6150.985789	0	0	0	0	0
6593.188271	0	0	0	0	0
7067.181274	0	0	0	0	0
7575.250259	0	0	0	0	0
8119.844993	0	0	0	0	0
8703.591361	0	0	0	0	0
9329.304026	0	0	0	0	0
10,000	0	0	0	0	0

Relaxtion time	Signal amplitude				
	Bound water	After water imbibition	After water-flooding	After oil-imbibition	After oil-flooding
B (d): NMR logs for sample 4					
0.01	0	0	0	0	0
0.010719	0	0	0	0	0
0.01149	0.000001091	0.000001	0.000001	0.000001	0.000001
0.012316	0.000004364	0.000004	0.000004	0.000003	0.000003
0.013201	0.000014183	0.000013	0.000013	0.000012	0.00001
0.01415	0.000048004	0.000044	0.000046	0.000041	0.000035
0.015167	0.000149467	0.000137	0.000142	0.000127	0.000109
0.016258	0.000430945	0.000395	0.000411	0.000366	0.000314
0.017426	0.001159733	0.001063	0.001106	0.000986	0.000846
0.018679	0.002864966	0.002626	0.002732	0.002435	0.00209
0.020022	0.006664919	0.006109	0.006354	0.005664	0.004861
0.021461	0.014647766	0.013426	0.013965	0.01245	0.010684
0.023004	0.030074506	0.027566	0.028672	0.025561	0.021935
0.024658	0.05885945	0.05395	0.056116	0.050026	0.04293
0.026431	0.110126631	0.100941	0.104992	0.093599	0.080323
0.028331	0.197513549	0.181039	0.188304	0.167873	0.144063

Relaxtion time	Signal amplitude				
	Bound water	After water imbibition	After water-flooding	After oil-imbibition	After oil-flooding
0.030368	0.336601866	0.308526	0.320902	0.286093	0.245521
0.032551	0.547631814	0.501954	0.522079	0.465472	0.399472
0.034891	0.871191866	0.798526	0.830512	0.740524	0.635557
0.037399	1.318100378	1.208158	1.256484	1.120485	0.961732
0.040088	2.026972173	1.857903	1.932061	1.723271	1.479284
0.04297	3.078913282	2.822102	2.934396	2.618019	2.247722
0.046059	4.506227124	4.130364	4.293993	3.832534	3.291221
0.04937	6.424405868	5.888548	6.120405	5.465608	4.695131
0.05292	9.013864911	8.262021	8.584632	7.671702	6.593026
0.056724	12.25729881	11.234921	11.66876	10.437606	8.974959
0.060802	16.31933838	14.958147	15.527355	13.905646	11.96534
0.065173	21.47811006	19.686627	20.421635	18.31597	15.773879
0.069859	27.52888225	25.232706	26.151961	23.498161	20.258037
0.074881	34.96626961	32.049743	33.181334	29.879492	25.791597
0.080264	43.36919853	39.751786	41.100474	37.106395	32.076481
0.086035	53.01018115	48.588617	50.155753	45.418114	39.327314
0.09222	64.4075603	59.035344	60.820696	55.26606	47.945311
0.09885	76.67919813	70.283408	72.240914	65.900296	57.291693
0.105956	90.89731524	83.315596	85.401678	78.247232	68.183836
0.113573	105.7815249	96.958318	99.068089	91.208836	79.679195
0.121738	121.8601745	111.695852	113.703591	105.239397	92.185849
0.13049	140.0634408	128.380789	130.132946	121.140506	106.421601
0.139871	158.41965	145.205912	146.476051	137.201365	120.899358
0.149927	177.7180599	162.894647	163.423532	154.092472	136.218773
0.160705	199.2212978	182.604306	182.080014	172.894902	153.351155
0.172259	220.1853865	201.819786	199.878834	191.209766	170.183961
0.184642	243.378985	223.078813	219.287848	211.418716	188.845099
0.197917	265.5072525	243.361368	237.278441	230.635939	206.770864
0.212145	287.9541269	263.935955	255.065314	250.038202	225.015311
0.227397	312.6280302	286.551815	274.28317	271.255997	245.05816
0.243744	335.4294905	307.451412	291.283612	290.705617	263.673267
0.261268	358.1466634	328.273752	307.627533	309.916883	282.23955
0.28005	383.0766309	351.124318	325.246464	330.852826	302.554194
0.300184	405.3569904	371.546279	339.976566	349.291281	320.764508
0.321764	429.8515747	393.997777	355.914469	369.41157	340.700441
0.344896	451.2092427	413.574008	368.606267	386.597639	358.110658
0.369691	471.8932837	432.532799	380.13578	402.966558	374.933056
0.396269	494.7905971	453.520254	392.816972	420.97242	393.454193
0.424757	513.9336181	471.066561	401.905837	435.529983	408.922847
0.455294	532.1420895	487.756269	409.71216	449.05396	423.573568
0.488025	552.5822483	506.49152	418.676158	464.214065	439.922669
0.52311	568.7926656	521.349831	423.90821	475.582628	452.82261
0.560717	587.2718229	538.287647	430.338497	488.620462	467.443179
0.601028	601.2773805	551.125005	433.037799	497.722617	478.414284
0.644236	614.1132529	562.890241	434.526333	505.673483	488.363788
0.690551	629.2833385	576.794994	437.298093	515.366212	500.073548
0.740196	639.7743486	586.410952	436.495256	521.066271	507.96504
0.79341	649.084348	594.944407	434.654321	525.680475	514.81707
0.850449	660.8226603	605.70363	434.208884	532.142843	523.485965

Relaxtion time	Signal amplitude				
	Bound water	After water imbibition	After water-flooding	After oil-imbibition	After oil-flooding
0.911589	667.8315814	612.127939	430.472436	534.701001	528.295114
0.977124	677.3530101	620.855188	428.219003	539.198296	534.974652
1.047371	682.1692187	625.269678	422.901155	539.901519	537.818866
1.122668	685.9543701	628.739111	416.944581	539.781009	539.736173
1.203378	692.3626226	634.612853	412.583819	541.724714	543.600358
1.28989	694.2045874	636.30118	405.546626	540.119509	543.767874
1.382622	695.1617511	637.178507	398.120583	537.888395	543.146246
1.482021	698.8340953	640.544542	392.375024	537.82653	544.554861
1.588565	698.1402793	639.908597	384.33877	534.491474	542.484724
1.702769	700.2172979	641.812372	378.021494	533.380778	542.507682
1.825183	701.5602447	643.043304	371.492022	531.812011	541.911654
1.956398	705.7236021	646.859397	366.629131	532.477043	543.45327
2.097046	709.2408836	650.083303	361.589107	532.740136	544.464444
2.247806	712.1488273	652.748696	356.412183	532.626768	544.98898
2.409404	714.4863614	654.891257	351.13181	532.156099	545.068796
2.582619	716.294456	656.548539	345.774139	531.340493	544.742696
2.768287	717.6157214	657.759598	340.357624	530.185195	544.04519
2.967302	718.4937266	658.564369	334.892767	528.68817	543.005391
3.180626	718.9720483	659.002794	329.382035	526.840143	541.64602
3.409285	719.0931165	659.113764	323.819978	524.62483	539.982558
3.654383	718.8969373	658.933948	318.193589	522.019412	538.022583
3.917101	718.4197873	658.496597	312.482915	518.995247	535.765356
4.198707	717.6929959	657.830427	306.661943	515.518839	533.2017
4.500558	716.741897	656.958659	300.699739	511.55303	530.314218
4.824109	715.5850377	655.898293	294.561821	507.058408	527.077876
5.17092	714.2336814	654.659653	288.211711	501.99485	523.46097
5.542665	712.6916271	653.246221	281.612595	496.323154	519.426447
5.941134	710.9553464	651.654763	274.729024	490.006678	514.933545
6.36825	709.0144094	649.875719	267.52856	483.012908	509.939674
6.826072	706.85215	647.893813	259.983301	475.314895	504.402462
7.316807	704.4465354	645.68885	252.071225	466.892514	498.281846
7.842822	701.7711731	643.236639	243.777298	457.733502	491.542124
8.406653	698.7964144	640.510004	235.094331	447.834267	484.153847
9.011018	695.4904836	637.47982	226.023573	437.200458	476.095473
9.658832	691.8206084	634.116048	216.575053	425.847305	467.354695
10.353218	687.7540804	630.388708	206.767673	413.799729	457.929416
11.097525	683.2592346	626.268776	196.629086	401.092232	447.828312
11.895341	678.3062997	621.728964	186.19537	387.76857	437.071016
12.750512	672.8681142	616.744376	175.510515	373.881207	425.687917
13.667164	666.9206968	611.293031	164.625733	359.490556	413.71963
14.649714	660.4436862	605.356266	153.59861	344.664024	401.216174
15.702901	653.4206541	598.919023	142.492107	329.474868	388.235927
16.831804	645.8393344	591.970059	131.373427	314.000901	374.844395
18.041864	637.6917769	584.502087	120.312774	298.323095	361.112855
19.338918	628.97446	576.511879	109.38201	282.524127	347.116902
20.729218	619.6883589	568.000329	98.653249	266.686938	332.934943
22.219469	609.8389844	558.972488	88.197419	250.893346	318.646669
23.816856	599.4363561	549.43754	78.08281	235.222787	304.331536
25.529081	588.4949157	539.408722	68.37366	219.751193	290.067285

Relaxtion time	Signal amplitude				
	Bound water	After water imbibition	After water-flooding	After oil-imbibition	After oil-flooding
27.3644	577.0333301	528.903144	59.128817	204.550045	275.928547
29.331663	565.0741885	517.941511	50.400523	189.685592	261.985572
31.440355	552.6435909	506.547746	42.233367	175.218211	248.303106
33.700643	539.7706408	494.748525	34.663457	161.201908	234.939468
36.123427	526.4868899	482.572768	27.717837	147.683887	221.945836
38.720388	512.8257828	470.05113	21.414179	134.7042	209.365753
41.504048	498.8221847	457.215568	15.760763	122.295431	197.234857
44.487828	484.512009	444.099	10.756712	110.482405	185.580819
47.686117	469.9320246	430.735128	9.672276	99.281925	174.42345
51.114335	455.1198242	417.158409	9.700432	88.702538	163.774974
54.789012	440.1139266	403.404149	9.958597	78.744331	153.640404
58.727866	424.9539699	389.50868	10.43358	69.398771	144.017997
62.94989	409.6808983	375.509531	11.109625	60.648615	134.899756
67.475441	394.3370416	361.445501	11.974127	52.467886	126.271922
72.326339	378.966007	347.35656	13.01531	44.82197	118.115449
77.525975	363.612293	333.283495	14.189308	37.667859	110.406414
83.099419	348.320573	319.267253	15.473727	30.954595	103.116349
89.073546	333.134644	305.347978	16.857396	25.24681	96.21249
95.477161	318.0960403	291.56374	18.305651	27.474104	89.657945
102.34114	303.2423874	277.949026	19.784064	29.687318	83.411802
109.69858	288.6055717	264.533063	21.275081	31.827319	77.42922
117.584955	274.2098409	251.338076	22.745114	33.822977	71.66154
126.038293	260.0699725	238.37761	24.150862	35.609925	66.056474
135.099352	246.1896454	225.655037	25.48489	37.132254	60.558422
144.811823	232.5601719	213.162394	26.697422	38.341142	55.108962
155.222536	219.1597112	200.879662	27.774606	39.220179	49.647548
166.381689	205.9530766	188.774589	28.703019	39.759088	44.112418
178.343088	192.8922116	176.803127	29.521621	39.896854	39.796602
191.164408	179.9173555	164.9105	30.135657	39.596567	41.599583
204.907469	166.9588939	153.0329	30.505352	38.808177	43.081097
219.638537	153.9397792	141.099706	30.561723	37.512646	44.169169
235.428641	140.7784451	129.036155	30.283337	35.705685	44.802604
252.353917	127.3920115	116.76628	29.628913	33.393769	44.933085
270.495973	113.6996222	104.215969	28.580379	30.592831	44.516982
289.942285	99.62571018	91.315958	27.137508	27.32738	43.523225
310.786619	85.10301969	78.004601	25.290199	23.62748	41.933214
333.129479	70.07521148	64.230258	23.046059	19.529152	39.739281
357.078596	54.49894775	49.953206	20.421932	15.075147	36.94316
382.749448	48.93407968	44.852502	17.446468	10.303808	33.556975
410.265811	47.9174226	43.920644	14.138874	5.255662	29.601193
439.760361	46.12815206	42.280616	10.531355	3.182175	25.104805
471.375313	43.55757931	39.924454	6.659408	2.95699	20.102968
505.263107	40.21327701	36.859099	3.831667	2.709244	14.636492
541.587138	36.11477731	33.102454	3.540841	2.446131	8.751329
580.522552	31.29441747	28.684159	3.209304	2.174275	4.455015
622.257084	25.79529416	23.643716	2.84729	1.899554	3.798291
666.991966	19.66803196	18.027527	2.464678	1.627013	3.042308
714.942899	12.97054443	11.888675	2.07066	1.360854	2.198428
766.341087	5.91614388	5.42268	1.673511	1.104462	1.278489

Relaxtion time	Signal amplitude				
	Bound water	After water imbibition	After water-flooding	After oil-imbibition	After oil-flooding
821.434358	3.570106575	3.272325	1.280469	0.860454	0.294416
880.488358	0.96093098	0.88078	0.897666	0.630757	0
943.787828	0	0	0.530131	0.416687	0
1011.63798	0	0	0.181827	0.219027	0
1084.365969	0	0	0	0.038115	0
1162.322469	0	0	0	0	0
1245.883364	0	0	0	0	0
1335.451563	0	0	0	0	0
1431.458938	0	0	0	0	0
1534.368409	0	0	0	0	0
1644.676178	0	0	0	0	0
1762.914118	0	0	0	0	0
1889.65234	0	0	0	0	0
2025.501939	0	0	0	0	0
2171.117946	0	0	0	0	0
2327.202479	0	0	0	0	0
2494.508135	0	0	0	0	0
2673.841616	0	0	0	0	0
2866.067617	0	0	0	0	0
3072.112999	0	0	0	0	0
3292.971255	0	0	0	0	0
3529.707303	0	0	0	0	0
3783.462617	0	0	0	0	0
4055.460736	0	0	0	0	0
4347.013158	0	0	0	0	0
4659.525669	0	0	0	0	0
4994.505116	0	0	0	0	0
5353.566677	0	0	0	0.02316	0
5738.441648	0	0	0	0.078077	0
6150.985789	0	0	0	0.134661	0
6593.188271	0	0	0.056348	0.190299	0
7067.181274	0	0	0.11993	0.244512	0
7575.250259	0	0	0.184168	0.297002	0
8119.844993	0	0	0.247286	0.347595	0
8703.591361	0	0	0.309051	0.470227	0
9329.304026	0	0	0.369849	0.609697	0
10,000	0	0	0.428215	0.741889	0

Declarations

Conflict of interest On behalf of all the co-authors, Shuwei Ma states that there is no conflict of interest.

References

Al-Dujaili AN, Shabani M, AL-Jawad MS (2023a) Lithofacies, deposition, and clinoforms characterization using detailed core data, nuclear magnetic resonance logs, and modular formation dynamics tests for Mishrif Formation Intervals in West Qurna/1 Oil Field, Iraq. SPE Res Eval Eng 26:1258–1270. https://doi.org/10.2118/214689-PA

Al-Dujaili AN, Shabani M, AL-Jawad MS (2023b) Effect of heterogeneity on recovery factor for carbonate reservoirs. A Case study for Mishrif formation in West Qurna Oilfield, Southern Iraq. Iraqi J Chem Petrol Eng 24(3):103–111. https://doi.org/10.31699/IJCPE.2023.3.10

Alessa S, Sakhaee-Pour A, Sadooni F, Al-Kuwari H (2021) Comprehensive pore size characterization of Midra shale. J Petrol Sci Eng 203:108576

Anderson W (1986) Wettability literature survey-part 2: wettability measurement. J Petrol Technol 38(11):1246–1262. https://doi.org/10.2118/13933-PA

Bobek JE, Mattax CC, Denekas MO (1958) Reservoir rock wettability-its significance and evaluation. Trans AIME 213(01):155–160. https://doi.org/10.2118/895-G

Borgia GC, Fantazzini P, Mesini E (1991) Wettability effects on oil-water-configurations in porous media: a nuclear magnetic resonance relaxation study. J Appl Phys 70(12):7623–7625. https://doi.org/10.1063/1.349720

Brown RJ, Fatt I (1956) Measurements of fractional wettability of oil fields' rocks by the nuclear magnetic relaxation method. https://doi.org/10.2118/743-G

Chen M, Dai J, Liu X, Kuang Y, Wang Z, Gou S et al (2020) Effect of displacement rates on fluid distributions and dynamics during water flooding in tight oil sandstone cores from nuclear magnetic resonance (NMR). J Petrol Sci Eng 184:106588

Tiab D, Donaldson EC (2004) Petrophysic, 2nd edn. Gulf Professional Publishing, Burlington

Donaldson EC, Thomas RD, Lorenz PB (1969) Wettability determination and its effect on recovery efficiency. Soc Petrol Eng J 9(01):13–20. https://doi.org/10.2118/2338-PA

Fu JH, Li SX, Xu LM, Niu XB (2018) Paleo-sedimentary environmental restoration and its significance of Chang 7 member of triassic Yanchang Formation in Ordos Basin, NW China. Petrol Explor Dev 45(6):936–946

Fu JH, Niu XB, Dan WD, Feng SB, Liang XW, Xin HG, You Y (2019) The geological characteristics and the progress on exploration and development of shale oil in Chang7 Member of Mesozoic Yanchang Formation, Ordos Basin. China Petrol Explor 24(5):601–614

Fu ST, Jin ZJ, Fu JH, Li SX, Yang WW (2021) Transformation of understanding from tight oil to shale oil in the Member 7 of Yanchang Formation in Ordos Basin and its significance of exploration and development. Acta Pet Sin 42(5):561–569

He G, Tang H (2011) Petrophysics. Petroleum Industry Press, Beijing, pp 240–242

Howard JJ (1998) Quantitative estimates of porous media wettability from proton NMR measurements. Magn Reson Imaging 16(5–6):529–533. https://doi.org/10.1016/S0730-725X(98)00060-5

Huang X, Dou L, Zuo X et al (2021) Dynamic imbibitionand drainage laws of fractures in tight reservoir. Act Petrolei Sinica 42(7):924–935

Jiao FZ (2021) FSV estimation and its application to development of shale oil via volume fracturing in the Ordos Basin. Oil Gas Geol 42(5):1181–1188

Kasha A, Sakhaee-Pour A, Hussein I (2022) Machine learning for capillary pressure estimation. SPE Reservoir Eval Eng 25(01):1–20

Minh CC, Crary S, Singer PM, Valori A, Bachman N, Hursan G et al (2015) Determination of wettability from magnetic resonance relaxation and diffusion measurements on fresh-state cores. In: SPWLA annual logging symposium, pp SPWLA-2015. SPWLA

Morrow NR (1990) Wettability and its effect on oil recovery. J Petrol Technol 42(12):1476–1484

National Development and Reform Commission (2007) Test method of reservoir rock wettability:SY/5153-2007. Petroleum Industry Press, Beijing

Sakhaee-Pour A, Bryant S (2012) Gas permeability of shale. SPE Reservoir Eval Eng 15(04):401–409

Sakhaee-Pour A, Bryant S (2015) Pore structure of shale. Fuel 143:467–475

Sakhaee-Pour A, Li W (2016) Fractal dimensions of shale. J Nat Gas Sci Eng 30:578–582

Sutanto E, Davis HT, Scriven LE (1990) Liquid distributions in porous rock examined by cryo scanning electron microscopy. SPE. https://doi.org/10.2118/20518-MS

Tran H, Sakhaee-Pour A (2018a) Slippage in shale based on acyclic pore model. Int J Heat Mass Transf 126:761–772

Tran H, Sakhaee-Pour A (2018b) Critical properties (Tc, Pc) of shale gas at the core scale. Int J Heat Mass Transf 127:579–588

Tran H, Sakhaee-Pour A (2019) The compressibility factor (Z) of shale gas at the core scale. Petrophysics 60(04):494–506

Wan X, Ma S, Fan J, Zhang Y, Zhang C (2023) Optimization of production system of shale oil development in Ordos basin, China. Sci Rep 13(1):6515. https://doi.org/10.1038/s41598-023-33080-8

Wang S, Javadpour F, Feng Q (2016) Molecular dynamics simulations of oil transport through inorganic nanopores in shale. Fuel 171:74–86. https://doi.org/10.1016/j.fuel.2015.12.071

Wang J, Xiao L, Liao G, Zhang Y, Guo L, Arns CH, Sun Z (2018) Theoretical investigation of heterogeneous wettability in porous media using NMR. Sci Rep 8(1):13450. https://doi.org/10.1038/s41598-018-31803-w

Washburn EW (1921) The dynamics of capillary flow. Phys Rev 17(3):273

Xiao W, Yang Y, Huang et al (2023). Rock wettability and its influence on crude oil producing characteristics based on NMR technology. Editorial Department of Petroleum Geology and Recovery Efficiency 30(1):112–121

Xiao W, Yang Y, Li M et al (2021) Experimental study on the oil production characteristics during the waterflooding of different types of reservoirs in Ordos Basin, NW China. Petrol Explor Dev 48(4):935–945. https://doi.org/10.1016/S1876-3804(21)60078-2

Xing H, Liangbin DOU, Xiongdi ZUO, Hui G, Tiantai L (2021) Dynamic imbibition and drainage laws of factures in tight reservoirs. Acta Petrolei Sinica 42(7):924. Dynamic imbibition and drainage laws of factures in tight reservoirs (syxb-cps.com.cn)

Yan J (2001) A new method for quantitative determination of rock wettability in oil reservoirs. Petrol Explor Dev 02:83–86+113–123

Yang T, Cao YC, Tian JC, Niu XB, Li SX, Zhou XP, Jin JH, Zhang YA (2021) Deposition of deep-water gravity-flow hybrid event beds in lacustrine basins and their sedimentological significance. Acta Geol Sin 95(12):3842–3857

Yang P, Guo H, Yang D (2013) Determination of residual oil distribution during waterflooding in tight oil formations with NMR relaxometry measurements. Energy Fuels 27(10):5750–5756. https://doi.org/10.1021/ef400631h

Yang Y, Xiao W, Liu S et al (2023) Characterization of pore throat heterogeneity in tight sandstone reservoirs and its impact on gas phase permeability. In: The 33rd national academic annual conference of natural gas. https://doi.org/10.26914/c.cnkihy.2023.071536

Yu C, Tran H, Sakhaee-Pour A (2018) Pore size of shale based on acyclic pore model. Transp Porous Media 124(2):345–368

Zapata Y, Sakhaee-Pour A (2016) Modeling adsorption-desorption hysteresis in shales: acyclic pore model. Fuel 181:557–565

Zhao T, Li X, Li M, Tang Y, Song L, He Y, Xing K (2021) Control of generalized capillary number on immiscible displacement path: NMR online and network simulation of fluid displacement mechanism. Energy Fuels 35(12):9903–9916. https://doi.org/10.1021/acs.energyfuels.1c00821

Zhiyu WU, Zhanwu GAO, Shuwei MA et al (2021) Preliminary study on imbibition and oil displacement of Chang 7 shale oil in Ordos Basin [J]. Natural Gas Geoscience 32(12):1874–1879

Zhong J, Wang P, Zhang Y, Yan Y, Hu S, Zhang J (2013) Adsorption mechanism of oil components on water-wet mineral surface: a molecular dynamics simulation study. Energy 59:295–300. https://doi.org/10.1016/j.energy.2013.07.016